Adiabatic coherent control in the anharmonic ion trap: Numerical analysis of vibrational anharmonicities

Lei Wang and Dmitri Babikov

Phys. Rev. A **83**, 022305 — Published 7 February 2011

DOI: 10.1103/PhysRevA.83.022305

Adiabatic Coherent Control in the Anharmonic Ion Trap: I. Numerical Analysis of Vibrational Anharmonicities

Lei Wang and Dmitri Babikov[1]

Chemistry Department, Marquette University, PO Box 1881, Milwaukee, Wisconsin, 53201

Abstract

Anharmonicity of the quantized motional states of ions in a Paul trap can be utilized to address the state-to-state transitions selectively and control the motional modes of trapped ions coherently and adiabatically [Zhao and Babikov, PRA 77, 12338, 2008]. In this paper we study two sources of the vibrational anharmonicity in the ion traps: the intrinsic Coulomb anharmonicity due to ion-ion interactions and the external anharmonicity of the trapping potential. Accurate numerical approach is used to compute energies and wavefunctions of vibrational eigenstates. Magnitude of the Coulomb anharmonicity is determined and shown to be insufficient for the successful control. In contrast, anharmonicity of the trapping potential allows controlling the motion of ions very efficiently using the time varying electric fields. Optimal control theory is used to derive the control pulses. One ion in a slightly anharmonic trap can be easily controlled. In the two- and three-ion systems the symmetric stretching mode is dark and cannot be controlled at all. The other two normal modes of the three-ion system can be controlled and used, for example, to encode a two-qubit system into the motional states of ions. A trap architecture that allows achieving the necessary amount of vibrational anharmonicity is proposed.

[1] Corresponding author: Dmitri.Babikov@mu.edu

1. Introduction

A new method for adiabatic coherent control of the quantized motional states of ions in a Paul trap was suggested recently by Zhao and Babikov [1]. They proposed to modify the harmonic trapping potential along the axial direction of the Paul trap in order to introduce small anharmonicity into the spectrum of collective motional/vibrational states of ions. When the spectrum of motional states is slightly anharmonic, different overtones occur at slightly different frequencies and the state-to-state transitions can, in principle, be controlled selectively by applying electric fields of appropriate frequency (in the MHz range), amplitude, duration and phase. In such control scenario all ions remain in the ground electronic state and the dynamics is adiabatic. The phase of motion can also be controlled [1], which makes this scheme potentially useful for coherent manipulations with ions and for quantum computation. For example, different qubits can be encoded into different normal vibration modes of the ion chain (*e.g.*, the center-of-mass motion mode and the asymmetric stretching mode) and addressed selectively using different frequencies. Addressing of individual ions is unnecessary. Note that such control scenario is quite different from the original approach of Cirac and Zoller [2], according to which the qubits are encoded in the *electronic* states of individual ions and manipulated using lasers [2-18]. Opportunity of using the vibrational states of ion chains for encoding qubits and the time varying electric fields for applying quantum gates is new and attractive and should be explored.

In Ref. [1] Zhao and Babikov considered the simplest case -- single ion in an anharmonic trap, and employed an approximate analytic model in order to introduce anharmonicity into the spectrum of motional states. The state-to-state transition moment matrix was described analytically and approximately. The optimal control theory (OCT) was employed to derive shaped pulses for several major quantum gates such as qubit flips, phase shifts, NOT and

Hadamard transform. They showed that the value of anharmonicity parameter on the order of 1% of the trap frequency is sufficient in order to obtain simply-shaped pulses optimized for accurate state-to-state transitions and for the quantum logics gates. Durations of predicted pulses were in the ten microsecond range; the field amplitudes were on the order of few mV/cm. It seems that the practical realization of this approach is within the reach of today's technology.

In this work we lift the assumptions of Zhao and Babikov and employ accurate numerically converged methods to study this new scheme of the adiabatic coherent control. We also go beyond the one-ion system and explore the control of two and three ions in several different trap architectures.

This paper is first in a series of two papers on this topic. Here (Paper I) we report results of numerical calculations of spectra of the motional states of ions in anharmonic traps and present analysis of their anharmonicities. It was emphasized in several earlier OCT studies [1, 19-22] that the vibrational anharmonicity is essential for successful control of the ground state dynamics (adiabatic control). Here we make connection between the shape of the trap and the resultant anharmonicity of the motional spectrum of ions. We show that the relationship between the shape of trapping potential and the anharmonicity of motional spectrum is simple only for one ion in a trap. The results for two and three ions in a trap are very interesting and some of them are quite unexpected [18]. The main outcome of this paper is our proposal for architecture of the trap which should provide anharmonicity of the spectrum (~ 1% of the vibration frequency) sufficient to achieve accurate control in the three-ion system, suitable to encode two qubits into the motional states of trapped ions. We have already carried out the OCT calculations of shaped pulses for major quantum gates in such vibrational two-qubit system. These results will be reported in the near future in the next paper of this series, Paper II, Ref. [23].

This paper is organized as follows. In Section 2 we study one ion in a trap; results of this section mainly confirm the findings of Ref. [1]. The effect of Coulomb anharmonicities is explored in a system of two ions in a trap, and is reported in Sec. 3 of the paper. Section 4 is dedicated to studies of three ions trapped in three different types of potential. Major findings are summarized as Conclusions in Sec. 5.

2. Single Ion in an Anharmonic Trap

In all models we considered in this work we assumed that the axial motion of ions is sufficiently decoupled from the other two degrees of freedom. Such approximation is enabled by large separation of the axial and radial frequencies of the trap -- conditions typical to many modern trap architectures. For one ion in a trap the problem is simply one-dimensional, with the model Hamiltonian operator for the axial motion along z given by:

$$\hat{H} = -\frac{1}{2m}\frac{d^2}{dz^2} + V_{\text{trap}}(z) \,. \tag{1}$$

Here m is mass of the ion and $V_{\text{trap}}(z)$ is the trapping potential along z-axis of the trap. The ion is assumed to be singly charged. The anharmonic trapping potential is taken in the following analytic form, which can be thought of as truncation to only first two symmetric terms of the Taylor series expansion:

$$V_{\text{trap}}(z) = k\frac{z^2}{2} + k'\frac{z^4}{4!} + \ldots \tag{2}$$

Here the coefficients k and k' are two force constants. For this model the numerical values of parameters were chosen to mimic the experiments in the group of Monroe [24-26], where the cadmium ions $^{111}Cd^{+}$ were trapped with the axial (harmonic) frequency $\omega/2\pi = 2.77$ MHz. The harmonic force constant was obtained as usual, $k = m\omega^2$. The coefficient k' controls

anharmonicity; if it is set to zero the system is harmonic with analytic solutions to energies and wave functions. The value of k' was varied in our model. Independent calculations were carried out with different values of k'. Finally, the value of $k'/2\pi = 1.067\times10^{-7}$ MHz/a_0^4 was chosen in order to provide the value of anharmonicity parameter $\Delta \sim 1\%$ of the trap frequency ω, close to the amount of anharmonicity used in the previous work, Ref. [1]. Everywhere in this paper we use the atomic unit of length, which is the Bohr radius, a_0.

Numerical calculations of vibrational states in this system are straightforward using the finite basis set representation approach (FBR). Since the system is only slightly anharmonic the orthonormal basis set of the harmonic oscillator functions, $\varphi_i(z)$, is a convenient choice. Matrix elements of the kinetic energy operator can be obtained analytically [27]:

$$T_{i,j} = -\frac{k}{4\alpha^2}[4\sqrt{j(j-1)}\delta_{i,j-2} - 4\sqrt{j}(\sqrt{i+1}\delta_{i,j-2} + \sqrt{i}\delta_{i,j}) - 2\delta_{i,j}$$

$$+ ((2i+1)\delta_{i,j} + \sqrt{(i+1)(i+2)}\delta_{i,j-2})], \qquad (3)$$

where $\alpha = \sqrt{m\omega} = \sqrt{k/\omega}$. Matrix elements of the potential energy function

$$V_{i,j} = \left\langle \varphi_j(z) \middle| \frac{1}{2}kz^2 + \frac{1}{4!}k'z^4 \middle| \varphi_i(z) \right\rangle \qquad (4)$$

were computed numerically using large quadrature of the equally spaced points. Convergence studies were carried out in order to determine the appropriate range of integration and the number of points. The range from $z^{\min} = -650\ a_0$ to $z^{\max} = +650\ a_0$ and the number of points $M = 131$ were finally adopted (leading to the integration step size $\Delta z = 10\ a_0$). For comparison, the distance of 650 a_0 equals to 34.4 nm.

The Hamiltonian matrix was diagonolized using DSYEV subroutine of ACML library [28]. All calculations of this paper were carried out at the NERSC center [29]. Careful

convergence studies with respect to the basis set size were conducted. We found that $N = 20$ basis functions are sufficient to compute energies of the vibrational states up to $|v = 10\rangle$ with accuracy better than 10^{-9} MHz. Energy eigenvalues, E, for the lowest eleven states, assigned the vibrational quantum numbers v, are presented in Table 1. Their deviations from analytic states of the harmonic ($k' = 0$) potential, computed as

$$\delta E = E - E_{harm}, \tag{5}$$

where

$$E_{harm} = \omega\left(v + \frac{1}{2}\right), \tag{6}$$

are also given in Table 1 and are presented in Fig. 1. The parabolic trend in Fig. 1 demonstrates clearly that the spectrum of states calculated numerically for the $k' \neq 0$ case is anharmonic.

In order to quantify the effect of anharmonicity, we used the numerical values of energies of three lowest states in the anharmonic potential (v = 0, 1 and 2 from Table 1) to derive coefficients of the analytic Dunham expansion [30]:

$$E_v = D + \omega\left(v + \frac{1}{2}\right) - \Delta\left(v + \frac{1}{2}\right)^2. \tag{7}$$

We obtained:

$$\omega/2\pi = 2.771 \text{ MHz},$$

$$\Delta/2\pi = -2.179\times10^{-2} \text{ MHz},$$

$$D/2\pi = -5.214\times10^{-3} \text{ MHz}.$$

These data show that the value of anharmonicity parameter, Δ, is close to 1% of the trap frequency. The value of ω from this fit is very close to the harmonic frequency (within the

effect of small anharmonicity). Overall, the Dunham expansion describes relatively well the low energy part of spectrum in the anharmonic ion trap.

Note that for the OCT calculations of Ref. [1] the approximate (analytic model) values of energies and matrix elements were used. Accurate (numerically converged) results obtained here gave us opportunity to check the results of Ref. [1]. Thus, using energies and wave functions obtained here we computed the transition moment matrix numerically and repeated all the OCT calculations of Ref. [1] for the qubit encoded into the $|v=0\rangle$ and $|v=1\rangle$ motional states of one ion in the anharmonic trap. The pulses optimized here for the gates NOT and Hadamard looked very similar to those obtained in Ref. [1]. The gate fidelities achieved with these pulses were nearly 0.9999, consistent with Ref. [1]. This comparison confirms rigorously the results of Ref. [1].

The conclusion here is that by modifying the trap potential (making it slightly anharmonic) it is relatively easy to achieve control over the vabrational states of one single ion in a Paul trap.

3. Two Ions in a Trap

When two or more ions are placed into a trap their Coulomb interaction introduces some anharmonicity, even if the trapping potential is purely harmonic ($k'=0$). The purpose of this section is to quantify the effect of this intrinsic Coulomb anharmonicity onto the spectrum of vibrational states and to determine whether or not it is sufficient for the control of the ground state dynamics in a purely harmonic potential.

For two ions in a linear harmonic trap the potential energy function is (in atomic units):

$$V(z_1, z_2) = V_{\text{trap}}(z_1, z_2) + \frac{1}{|z_2 - z_1|} = k\frac{z_1^2}{2} + k\frac{z_2^2}{2} + \frac{1}{|z_2 - z_1|}, \qquad (8)$$

where z_1 and z_2 are Cartesian coordinates for positions of two ions. In the molecular dynamics calculations a two-dimensional potential energy function, such as one in Eq. (8), is called the potential energy surface (PES) and is often presented and analyzed using a color map, such as one given in Fig. 2. Color in this picture shows the value of potential energy, with violet color corresponding to low energy and red color corresponding to high energy. White area along the diagonal of this picture describes arrangements with $z_1 \approx z_2$, where the two ions are close together and the energy is very large due to Coulomb repulsion. This picture demonstrates clearly that the overall PES is very anharmonic. Two minima in Fig. 2 describe two equivalent arrangements: $z_1 < z_2$ and $z_2 < z_1$; we can focus on only one of these wells and we chose the one with $z_1 < z_2$.

The first step in our procedure is to find the equilibrium positions of the two ions in a trap, *i.e.*, to locate the minimum energy point on the PES of Fig. 2. For this purpose we employed the *Newton-Raphson* minimization method [31, 32]. For the trap parameters introduced above we obtained $z_1^{eq} = -5.610 \times 10^3\ a_0$ and $z_2^{eq} = 5.610 \times 10^3\ a_0$. The value of potential energy at this point was $V^{eq}/2\pi = V(z_1^{eq}, z_2^{eq})/2\pi = 1.340 \times 10^5$ MHz.

The second step of our procedure is the normal mode analysis near the equilibrium point. The Hessian matrix at the equilibrium point can be constructed analytically using Eq. (9) in Cartesian coordinates [31, 32]:

$$\mathbf{F} = \begin{vmatrix} m & 0 \\ 0 & m \end{vmatrix}^{-1/2} \begin{vmatrix} \dfrac{\partial^2 V}{\partial z_1^2} & \dfrac{\partial^2 V}{\partial z_1 \partial z_2} \\ \dfrac{\partial^2 V}{\partial z_2 \partial z_1} & \dfrac{\partial^2 V}{\partial z_2^2} \end{vmatrix} \begin{vmatrix} m & 0 \\ 0 & m \end{vmatrix}^{-1/2} \tag{9}$$

Diagonalization of the Hessian matrix gives two normal mode frequencies:

$$\omega_1 / 2\pi = 2.770 \text{ MHz},$$

$$\omega_2 / 2\pi = 4.798 \text{ MHz},$$

and their corresponding eigenvectors:

$$\mathbf{A} = \begin{vmatrix} a_{11} & a_{12} \\ a_{21} & a_{22} \end{vmatrix} = \begin{vmatrix} \dfrac{\sqrt{2}}{2} & \dfrac{\sqrt{2}}{2} \\ \dfrac{\sqrt{2}}{2} & -\dfrac{\sqrt{2}}{2} \end{vmatrix} \approx \begin{vmatrix} 0.7071 & 0.7071 \\ 0.7071 & -0.7071 \end{vmatrix}. \tag{10}$$

These two vibration modes are familiar center-of-mass motion mode with $a_{11} = a_{21}$ (Mode 1) and the symmetric stretching mode with $a_{12} = -a_{22}$ (Mode 2). Note that here for two (and in the next Section for three) ions this step can be carried out either analytically or numerically. For four and more ions (in the future work) the numerical procedure is required. In order to test our computer codes we did both numerical and analytic diagonalization and obtained equivalent results.

The third step is to transform the Hamiltonian operator from the Cartesian coordinates,

$$\hat{H}(z_1, z_2) = -\frac{1}{2m}\frac{\partial^2}{\partial z_1^{\,2}} - \frac{1}{2m}\frac{\partial^2}{\partial z_2^{\,2}} + V(z_1, z_2) - V^{eq}, \tag{11}$$

into the normal mode coordinates. This is needed in order to use a simple direct-product basis set of one-dimensional Harmonic oscillator functions for the numerical solution of the two-dimensional Schrödinger equation. In Eq. (11) the potential energy operator $V(z_1, z_2)$ is from Eq. (8). Note that we introduced the constant energy shift into the Hamiltonian in order to account

for large Coulomb repulsion energy associated with the equilibrium (energy minimum) configuration.

We introduce the mass-scaled coordinates $\bar{z}_i$, the corresponding displacement coordinates $\Delta\bar{z}_i$, and the normal mode coordinates $\bar{\zeta}_i$ as follows:

$$\bar{z}_1 = \sqrt{m} z_1, \qquad \bar{z}_2 = \sqrt{m} z_2, \tag{12}$$

$$\begin{cases} \bar{z}_1 - \sqrt{m} z_1^{eq} = \Delta\bar{z}_1 \\ \bar{z}_2 - \sqrt{m} z_2^{eq} = \Delta\bar{z}_2 \end{cases}, \tag{13}$$

$$\begin{vmatrix} \Delta\bar{z}_1 \\ \Delta\bar{z}_2 \end{vmatrix} = \begin{vmatrix} a_{11} & a_{12} \\ a_{21} & a_{22} \end{vmatrix} \begin{vmatrix} \bar{\zeta}_1 \\ \bar{\zeta}_2 \end{vmatrix}. \tag{14}$$

In these mass scaled normal mode coordinates the Hamiltonian operator is expressed as:

$$\hat{H}(\bar{\zeta}_1, \bar{\zeta}_2) = -\frac{1}{2}\frac{\partial^2}{\partial \bar{\zeta}_1^{\,2}} - \frac{1}{2}\frac{\partial^2}{\partial \bar{\zeta}_2^{\,2}} + V(\bar{\zeta}_1, \bar{\zeta}_2) - V^{eq}, \tag{15}$$

$$V(\bar{\zeta}_1, \bar{\zeta}_2) = \frac{1}{2}k\left(z_1^{eq} - \frac{\bar{\zeta}_1 + \bar{\zeta}_2}{\sqrt{2m}}\right)^2 + \frac{1}{2}k\left(z_2^{eq} + \frac{\bar{\zeta}_2 - \bar{\zeta}_1}{\sqrt{2m}}\right)^2 + \frac{1}{\left|\frac{2\bar{\zeta}_2}{\sqrt{2m}} + (z_2^{eq} - z_1^{eq})\right|}. \tag{16}$$

3.a. Harmonic Approximation

It is instructive to consider an approximation to this Hamiltonian, which allows solving the Schrödinger equation analytically and approximately. Note that the Coulomb interaction is included only into the last term of Eq. (16). This term is clearly anharmonic and depends only on the symmetric stretching coordinate $\bar{\zeta}_2$. If this term is expanded into the Taylor series and all terms beyond quadratic in $\bar{\zeta}_2$ are neglected, we obtain:

$$V(\bar{\zeta}_1, \bar{\zeta}_2) = \frac{1}{2}\frac{k}{m}\bar{\zeta}_1^{\,2} + \frac{1}{2}\frac{k}{m}\bar{\zeta}_2^{\,2} + \frac{k\bar{\zeta}_2(z_2^{eq} - z_1^{eq})}{\sqrt{2m}} + \frac{k}{2}(z_1^{eq\,2} + z_2^{eq\,2})$$

$$+\frac{1}{(z_2^{eq}-z_1^{eq})}-\frac{2}{\sqrt{2m}(z_2^{eq}-z_1^{eq})^2}\bar{\zeta}_2+\frac{4}{2m(z_2^{eq}-z_1^{eq})^3}\bar{\zeta}_2^{\,2}+... \tag{17}$$

From this expression, using properties of the equilibrium point ($\bar{\zeta}_1=\bar{\zeta}_2=0$, $-z_1^{eq}=z_2^{eq}$ and $\partial V/\partial z^{eq}=0$) we can obtain approximate analytical expressions for the equilibrium positions (in the harmonic approximation):

$$z_1^{eq}=-\left(\frac{1}{4k}\right)^{1/3}, \tag{18}$$

$$z_2^{eq}=\left(\frac{1}{4k}\right)^{1/3}, \tag{19}$$

and for the equilibrium energy (in the harmonic approximation):

$$V^{eq}=V(z_1^{eq},z_2^{eq})=\frac{3}{2}\left(\frac{k}{2}\right)^{1/3}. \tag{20}$$

Using Eqs. (15, 17, 18, 19, 20) the Hamiltonian can be presented in the following form (in the harmonic approximation):

$$\hat{H}(\bar{\zeta}_1,\bar{\zeta}_2)=-\frac{1}{2}\frac{\partial^2}{\partial\bar{\zeta}_1^{\,2}}-\frac{1}{2}\frac{\partial^2}{\partial\bar{\zeta}_2^{\,2}}+\frac{1}{2}\frac{k}{m}\bar{\zeta}_1^{\,2}+\frac{1}{2}\frac{3k}{m}\bar{\zeta}_2^{\,2}$$

$$=-\frac{1}{2}\frac{\partial^2}{\partial\bar{\zeta}_1^{\,2}}-\frac{1}{2}\frac{\partial^2}{\partial\bar{\zeta}_2^{\,2}}+\frac{1}{2}k\left(\frac{\bar{\zeta}_1}{\sqrt{m}}\right)^2+\frac{1}{2}k\left(\sqrt{\frac{3}{m}}\bar{\zeta}_2\right)^2. \tag{21}$$

This approximate Hamiltonian operator is separable in $\bar{\zeta}_1$ and $\bar{\zeta}_2$ (two uncoupled harmonic oscillators) and has analytic solutions to energies and wave functions. We found it convenient to introduce the "unscaled" normal mode coordinates ζ_1 and ζ_2 (measured in the units of length, a_0) according to the following equation:

$$\begin{cases} \overline{\zeta}_1 = \sqrt{m}\zeta_1 \\ \overline{\zeta}_2 = \sqrt{\dfrac{m}{3}}\zeta_2 \end{cases}. \tag{22}$$

In such unscaled coordinates the Hamiltonian is expressed simply as:

$$\hat{H}(\zeta_1, \zeta_2) = -\frac{1}{2m}\frac{\partial^2}{\partial \zeta_1^{\,2}} - \frac{1}{2\left(\dfrac{m}{3}\right)}\frac{\partial^2}{\partial \zeta_2^{\,2}} + \frac{1}{2}k\zeta_1^{\,2} + \frac{1}{2}k\zeta_2^{\,2}. \tag{23}$$

The Harmonic frequencies of two modes are (in the harmonic approximation):

$$\omega_1 = \sqrt{k/m} = \omega, \tag{24}$$

$$\omega_2 = \sqrt{k\Big/\left(\frac{m}{3}\right)} = \sqrt{3}\omega. \tag{25}$$

Using parameters of our model we obtained, in the harmonic approximation, $z_1^{eq} = -5.610\times10^3\, a_0$, $z_2^{eq} = 5.610\times10^3\, a_0$, $V^{eq}/2\pi = 1.340\times10^5$ MHz, $\omega_1/2\pi = 2.770$ MHz and $\omega_2/2\pi = 4.798$ MHz. These numbers are close to those obtained numerically at the beginning of this Section.

Note that analytical expressions of Eqs. (18, 19) for the equilibrium distances and Eqs. (24, 25) for the vibration frequencies, obtained here within the harmonic approximation, are consistent with results of James and coworkers [33, 34] obtained in a different way, and also with the NIST data [35]. This comparison provides an important benchmark for our theory and clearly demonstrates that the exact framework (beyond the harmonic approximation) developed in this work goes beyond the existing theoretical treatments of the ion chains in Paul traps.

3.b. Numerical Solution

Using conclusions of the discussion above it is convenient to rewrite the exact Hamiltonian of Eq. (15) using the mass-unscaled normal mode coordinates ζ_i. The resultant expression is:

$$\hat{H}(\zeta_1,\zeta_2) = -\frac{1}{2m}\frac{\partial^2}{\partial\zeta_1^{\,2}} - \frac{1}{2\left(\frac{m}{3}\right)}\frac{\partial^2}{\partial\zeta_2^{\,2}} + V(\zeta_1,\zeta_2) - V^{eq}, \tag{26}$$

$$V(\zeta_1,\zeta_2) = \frac{1}{2}k\left(z_1^{eq} - \frac{\sqrt{3}\zeta_1+\zeta_2}{\sqrt{6}}\right)^2 + \frac{1}{2}k\left(z_2^{eq} + \frac{\zeta_2-\sqrt{3}\zeta_1}{\sqrt{6}}\right)^2 + \frac{1}{\left|\sqrt{\frac{2}{3}}\zeta_2 + (z_2^{eq}-z_1^{eq})\right|}. \tag{27}$$

This expression is exact and contains all anharmonicities. It involves no approximations, just the transformation of coordinates. It is interesting that this full Hamiltonian is, in fact, also separable in ζ_1 and ζ_2 because the potential coupling terms proportional to the product $\zeta_1\times\zeta_2$ cancel each other due to properties of the normal mode eigenvectors, Eqs. (10, 14). The Mode 1 is completely uncoupled and can be solved analytically. The Mode 2 is more complicated because the Coulomb repulsion term depends on ζ_2. Note, however, that this separability is *not* general. In the next Section the cases will be presented where the modes are coupled and the exact Hamiltonian is not separable. Since our purpose was to treat such inseparable cases too, we did not make use of separability here and followed a brute-force general approach to solve the Schrödinger equation numerically. We expressed the wave function in (ζ_1,ζ_2)-coordinates and expanded it using the direct-product basis set of the harmonic oscillator functions with the normal mode frequencies ω_1 and ω_2 for the coordinates ζ_1 and ζ_2, respectively:

$$\psi_v(\zeta_1,\zeta_2) = \sum_{i,j}^{N} C_{v_{i,j}}\varphi_i(\zeta_1)\varphi_j(\zeta_2), \tag{28}$$

The basis set size was $N_1 \times N_2 = 15 \times 15$. The following parameters were used for numerical quadratures of the potential matrix elements: $\zeta_1^{\max} = \zeta_2^{\max} = 500\ a_0$, $M_1 = M_2 = 101$ ($\Delta\zeta_1 = \Delta\zeta_2 = 10\ a_0$). Convergence studies showed that with these parameters the accuracy of lowest 77 states is better than 10^{-9} MHz.

Some of the eigenvalues calculated numerically and their assignments in terms of the normal vibration mode quantum numbers are given in Table 2. In order to elucidate the effect of Coulomb anharmonicity, we computed deviations of the numerical spectrum from the Harmonic one, $\delta E = E - E_{harm}$, where

$$E_{harm} = \omega_1\left(v_1 + \frac{1}{2}\right) + \omega_2\left(v_2 + \frac{1}{2}\right). \tag{29}$$

Here ω_1 and ω_2 are frequencies obtained numerically from diagonalization of the Hessian matrix. The values of δE are given in Table 2 and are also presented in Fig. 3 for nine lowest states of each normal mode progression. Figure 3 shows very clearly that Mode 1 (center-of-mass motion of two ions) remains harmonic, while Mode 2 (symmetric stretching) shows a distinct effect of Coulomb anharmonicity.

This effect is easy to understand from general arguments. In Mode 1 two ions move together along the *z*-axis as a single pseudo-particle. Such simultaneous center-of-mass motion of two ions does not change the distance between them, and does not change the amount of Coulomb interaction. Excitation of the Mode 2, however, brings ions closer together and takes them further apart, changing the Coulomb repulsion energy of the system.

Alternatively, the same explanation can be derived from a quick glance at Eq. (27) for the potential energy operator, which shows that the Coulomb interaction term includes only ζ_2, but no ζ_1.

In order to quantify the effect of Coulomb anharmonicity we calculated the coefficients for the 2D-Dunham expansion [30]:

$$E_{v_1,v_2} = D + \omega_1\left(v_1+\frac{1}{2}\right) - \Delta_1\left(v_1+\frac{1}{2}\right)^2 + \omega_2\left(v_2+\frac{1}{2}\right) - \Delta_2\left(v_2+\frac{1}{2}\right)^2$$

$$- \Delta_{12}\left(v_1+\frac{1}{2}\right)\left(v_2+\frac{1}{2}\right), \qquad (30)$$

based on numerical values of six eigenstates (ground state, first exited states of each mode, their overtones, and the combination state). The results were:

$$D/2\pi = 6.280\times10^{-6}\ \text{MHz},$$

$$\omega_1/2\pi = 2.770\ \text{MHz},$$

$$\omega_2/2\pi = 4.798\ \text{MHz},$$

$$\Delta_1 \approx 0,$$

$$\Delta_2/2\pi = -6.851\times10^{-6}\ \text{MHz},$$

$$\Delta_{12} \approx 0.$$

From these data we see that although the Coulomb interaction introduces some anharmonicity into the spectrum of the symmetric stretching mode, the value of this anharmonicity is way too low for the control. The anharmonicity parameter in this case is $\Delta_2 \sim 10^{-6}\omega_2$, which is about four orders of magnitude smaller than is needed for the successful control.

We also encountered another fundamental problem that makes the symmetric stretching mode unsuitable for the scheme of control proposed in Ref. [1]. We will mention only briefly here, but will expand on this topic in the future publication, Paper II [23], that the proposal of Ref. [1] was to use the time-varying *spatially homogeneous* field for the control. It appears that, due to symmetry, all elements of the transition matrix for excitation of the symmetric stretching

mode appear to be zero, which means that this mode is "dark" and cannot be excited or controlled using spatially homogeneous electric fields. The symmetry properties of the transition moment matrix will be discussed in detail in Paper II [23]. (It should be possible, however, to control the symmetric stretching mode using *spatially inhomogeneous* fields. Creating the field gradients in the ion trap is trivial, but exploration of this opportunity goes beyond the scope of this paper.)

Based on these findings, we decided not to study the system of two ions trapped in an anharmonic potential. We expect that anharmonicity of the trapping potential would make the center-of-mass motion mode (Mode 1) anharmonic, similar to the one-ion case. The Mode 2, even if anharmonic, would remain dark anyway. Our conclusion for two ions is following: If the spatially homogeneous time varying field is used for control, the two-ion system offers no advantages compared to the one-ion case.

4. Three Ions in a Trap

The numerical procedure for three ions in a trap follows closely that of the previous section. Only the key points will be emphasized here. The potential energy function of the three-ion system is:

$$V(z_1, z_2, z_3) = V_{\text{trap}}(z_1, z_2, z_3) + \frac{1}{|z_2 - z_1|} + \frac{1}{|z_3 - z_1|} + \frac{1}{|z_3 - z_2|}, \tag{31}$$

where z_1, z_2 and z_3 are Cartesian coordinates of three ions. Three different analytic forms of V_{trap} were studied and are discussed separately further in this Section. For each V_{trap}, numerical minimization was carried out using the *Newton-Raphson* method in order to determine coordinates (z_1^{eq} , z_2^{eq} and z_3^{eq}) and energy (V^{eq}) of the equilibrium configuration. At the

equilibrium configuration a 3×3 Hessian matrix was constructed analytically and diagonalized numerically to obtain three normal mode frequencies (ω_1, ω_2 and ω_3) and their corresponding eigenvectors:

$$\mathbf{A} = \begin{vmatrix} a_{11} & a_{12} & a_{13} \\ a_{21} & a_{22} & a_{23} \\ a_{31} & a_{32} & a_{33} \end{vmatrix}. \tag{32}$$

The eigenvectors were used to transform the Hamiltonian from Cartesian coordinates to the normal mode coordinates:

$$\hat{H}(\bar{\zeta}_1, \bar{\zeta}_2, \bar{\zeta}_3) = -\frac{1}{2}\frac{\partial^2}{\partial \bar{\zeta}_1^{\,2}} - \frac{1}{2}\frac{\partial^2}{\partial \bar{\zeta}_2^{\,2}} - \frac{1}{2}\frac{\partial^2}{\partial \bar{\zeta}_3^{\,2}} + V(\bar{\zeta}_1, \bar{\zeta}_2, \bar{\zeta}_3) - V^{eq}, \tag{33}$$

$$V(\bar{\zeta}_1, \bar{\zeta}_2, \bar{\zeta}_3) = \frac{1}{2}k\left(\frac{a_{11}\bar{\zeta}_1 + a_{12}\bar{\zeta}_2 + a_{13}\bar{\zeta}_3}{\sqrt{m}} + z_1^{eq}\right)^2$$

$$+ \frac{1}{2}k\left(\frac{a_{21}\bar{\zeta}_1 + a_{22}\bar{\zeta}_2 + a_{23}\bar{\zeta}_3}{\sqrt{m}} + z_2^{eq}\right)^2 + \frac{1}{2}k\left(\frac{a_{31}\bar{\zeta}_1 + a_{32}\bar{\zeta}_2 + a_{33}\bar{\zeta}_3}{\sqrt{m}} + z_3^{eq}\right)^2$$

$$+ \frac{1}{\left|\dfrac{a_{21}\bar{\zeta}_1 + a_{22}\bar{\zeta}_2 + a_{23}\bar{\zeta}_3}{\sqrt{m}} - \dfrac{a_{11}\bar{\zeta}_1 + a_{12}\bar{\zeta}_2 + a_{13}\bar{\zeta}_3}{\sqrt{m}} + (z_2^{eq} - z_1^{eq})\right|}$$

$$+ \frac{1}{\left|\dfrac{a_{31}\bar{\zeta}_1 + a_{32}\bar{\zeta}_2 + a_{33}\bar{\zeta}_3}{\sqrt{m}} - \dfrac{a_{11}\bar{\zeta}_1 + a_{12}\bar{\zeta}_2 + a_{13}\bar{\zeta}_3}{\sqrt{m}} + (z_3^{eq} - z_1^{eq})\right|}$$

$$+ \frac{1}{\left|\dfrac{a_{31}\bar{\zeta}_1 + a_{32}\bar{\zeta}_2 + a_{33}\bar{\zeta}_3}{\sqrt{m}} - \dfrac{a_{21}\bar{\zeta}_1 + a_{22}\bar{\zeta}_2 + a_{23}\bar{\zeta}_3}{\sqrt{m}} + (z_3^{eq} - z_2^{eq})\right|}. \tag{34}$$

Finally, the following relations:

$$\begin{cases} \overline{\zeta}_1 = \sqrt{m}\zeta_1 \\ \overline{\zeta}_2 = \omega_1/\omega_2\sqrt{m}\zeta_2 \\ \overline{\zeta}_3 = \omega_1/\omega_3\sqrt{m}\zeta_3 \end{cases} \quad (35)$$

were used to transform Hamiltonian to the "unscaled" normal mode coordinates:

$$\hat{H}(\zeta_1,\zeta_2,\zeta_3) = -\frac{1}{2m}\frac{\partial^2}{\partial\zeta_1^{\,2}} - \frac{1}{2\left(\frac{\omega_1}{\omega_2}\right)^2 m}\frac{\partial^2}{\partial\zeta_2^{\,2}} - \frac{1}{2\left(\frac{\omega_1}{\omega_3}\right)^2 m}\frac{\partial^2}{\partial\zeta_3^{\,2}} + V(\zeta_1,\zeta_2,\zeta_3) - V^{eq}, \quad (36)$$

$$V(\zeta_1,\zeta_2,\zeta_3) = \frac{1}{2}k\omega_1^{\,2}\left(a_{11}\frac{\zeta_1}{\omega_1} + a_{12}\frac{\zeta_2}{\omega_2} + a_{13}\frac{\zeta_3}{\omega_3} + \frac{z_1^{eq}}{\omega_1}\right)^2$$

$$+\frac{1}{2}k\omega_1^{\,2}\left(a_{21}\frac{\zeta_1}{\omega_1} + a_{22}\frac{\zeta_2}{\omega_2} + a_{23}\frac{\zeta_3}{\omega_3} + \frac{z_2^{eq}}{\omega_1}\right)^2 + \frac{1}{2}k\omega_1^{\,2}\left(a_{31}\frac{\zeta_1}{\omega_1} + a_{32}\frac{\zeta_2}{\omega_2} + a_{33}\frac{\zeta_3}{\omega_3} + \frac{z_3^{eq}}{\omega_1}\right)^2$$

$$+\frac{1}{\omega_1\left|(a_{21}-a_{11})\frac{\zeta_1}{\omega_1} + (a_{22}-a_{12})\frac{\zeta_2}{\omega_2} + (a_{23}-a_{13})\frac{\zeta_3}{\omega_3} + \frac{z_2^{eq}-z_1^{eq}}{\omega_1}\right|}$$

$$+\frac{1}{\omega_1\left|(a_{31}-a_{11})\frac{\zeta_1}{\omega_1} + (a_{32}-a_{12})\frac{\zeta_2}{\omega_2} + (a_{33}-a_{13})\frac{\zeta_3}{\omega_3} + \frac{z_3^{eq}-z_1^{eq}}{\omega_1}\right|}$$

$$+\frac{1}{\omega_1\left|(a_{31}-a_{21})\frac{\zeta_1}{\omega_1} + (a_{32}-a_{22})\frac{\zeta_2}{\omega_2} + (a_{33}-a_{23})\frac{\zeta_3}{\omega_3} + \frac{z_3^{eq}-z_2^{eq}}{\omega_1}\right|}. \quad (37)$$

Three-dimensional wave function of the system was expressed in these $(\zeta_1,\zeta_2,\zeta_3)$-coordinates and was expanded using the direct-product basis set of the one-dimensional harmonic oscillator functions with the frequencies ω_1, ω_2 and ω_3 for ζ_1, ζ_2 and ζ_3, respectively:

$$\psi_v(\zeta_1,\zeta_2,\zeta_3) = \sum_{i,j,l}^{N} C_{v_{i,j,l}}\varphi_i(\zeta_1)\varphi_j(\zeta_2)\varphi_l(\zeta_3). \quad (38)$$

The eigenvalues were obtained numerically by diagonalizing the Hamiltonian matrix in this basis. In order to make the three-ion case numerically manageable we employed the Gaussian quadrature to calculate the matrix elements of the potential energy operator more efficiently [36] and used the Message Passing Interface (MPI) to parallelize the calculations [37]. The calculations for three ions were run using 16 processors of Franklin computer at NERCS [29], the run time for an average job was about 6 wall-clock hours. The normal mode quantum numbers were assigned based on shapes of wave functions. The spectrum was analyzed by computing $\delta E = E - E_{harm}$ with

$$E_{harm} = \omega_1\left(v_1 + \frac{1}{2}\right) + \omega_2\left(v_2 + \frac{1}{2}\right) + \omega_3\left(v_3 + \frac{1}{2}\right), \tag{39}$$

where ω_1, ω_2 and ω_3 are the normal mode frequencies obtained from diagonalization of Hessian matrix. Also, for each computed spectrum, we derived a set of ten coefficients of the 3D-Dunham expansion [30]:

$$E_{v_1,v_2,v_3} = D + \omega_1\left(v_1 + \frac{1}{2}\right) - \Delta_1\left(v_1 + \frac{1}{2}\right)^2 + \omega_2\left(v_2 + \frac{1}{2}\right) - \Delta_2\left(v_2 + \frac{1}{2}\right)^2 + \omega_3\left(v_3 + \frac{1}{2}\right) - \Delta_3\left(v_3 + \frac{1}{2}\right)^2$$

$$- \Delta_{12}\left(v_1 + \frac{1}{2}\right)\left(v_2 + \frac{1}{2}\right) - \Delta_{13}\left(v_1 + \frac{1}{2}\right)\left(v_3 + \frac{1}{2}\right) - \Delta_{23}\left(v_2 + \frac{1}{2}\right)\left(v_3 + \frac{1}{2}\right). \tag{40}$$

For this purpose we used ten numerically computed eigenvalues: the ground state, first excited state and the overtone for each mode, and three possible combination states.

4.a. Harmonic Trap

When the trapping potential is harmonic the first term in Eq. (31) has the form of

$$V_{\text{trap}}(z_1, z_2, z_3) = k\frac{z_1^2}{2} + k\frac{z_2^2}{2} + k\frac{z_3^2}{2}. \tag{41}$$

The PES for this case is shown in Fig. 4 using Cartesian coordinates. As before, white areas correspond to the regions of strong Coulomb repulsion and occur when two ions approach each other. For the well defined by $z_3 > z_2 > z_1$ numerical minimization gave $z_1^{eq} = -9.593\times10^3\, a_0$, $z_2^{eq} \approx 0$, $z_3^{eq} = 9.593\times10^3\ a_0$ and $V^{eq}/2\pi = V(z_1^{eq}, z_2^{eq}, z_3^{eq})/2\pi = 4.093\times10^5$ MHz. Diagonalization of the Hessian matrix gave the following frequencies of normal modes:

$$\omega_1/2\pi = 2.770 \text{ MHz},$$

$$\omega_2/2\pi = 4.798 \text{ MHz},$$

$$\omega_3/2\pi = 6.671 \text{ MHz},$$

with their corresponding eigenvectors:

$$\mathbf{A} = \begin{vmatrix} 0.5774 & 0.7071 & -0.4083 \\ 0.5774 & 0.0000 & 0.8165 \\ 0.5774 & -0.7071 & -0.4083 \end{vmatrix}. \tag{42}$$

These numbers describe the three familiar normal modes: Mode 1 with $a_{11} = a_{21} = a_{31}$ is the center-of-mass motion mode, Mode 2 with $a_{12} = -a_{32}$ and $a_{22} = 0$ is the symmetric stretching mode, and Mode 3 with $2a_{13} = -a_{23} = 2a_{33}$ is the asymmetric stretching mode. This information can be used to analytically simplify the anharmonic part of the potential energy function (last three terms in Eq. (37)). It is easy to show that the property $a_{11} = a_{21} = a_{31}$ leads to complete cancellation of all terms containing ζ_1, only the terms containing ζ_2 and ζ_3 remain in the anharmonic terms of the PES:

$$[Coulomb\ \ terms] = \frac{1}{\omega_1 \left| -a_{12}\frac{\zeta_2}{\omega_2} + (a_{23} - a_{13})\frac{\zeta_3}{\omega_3} + \frac{z_2^{eq} - z_1^{eq}}{\omega_1} \right|}$$

$$+\frac{1}{\omega_1\left|(a_{32}-a_{12})\dfrac{\zeta_2}{\omega_2}+\dfrac{z_3^{eq}-z_1^{eq}}{\omega_1}\right|}+\frac{1}{\omega_1\left|a_{32}\dfrac{\zeta_2}{\omega_2}+(a_{33}-a_{23})\dfrac{\zeta_3}{\omega_3}+\dfrac{z_3^{eq}-z_2^{eq}}{\omega_1}\right|}. \quad (43)$$

This transformation demonstrates analytically that the Mode 1 is uncoupled and is harmonic, while the Modes 2 and 3 are anharmonic (consistent with general arguments) and are coupled by the PES.

In fact, the same conclusion can be obtained by analyzing the picture of potential energy surface in the normal mode coordinates presented in Fig. 5. Note that white area on the picture goes parallel to the ζ_1-axis. Recall that in this (white) area of the configuration space the Coulomb repulsion become very large. Figure 5 shows that excitation of Mode 1 does not bring the system closer to the white area, which suggests that Mode 1 must be harmonic. However, the motion along ζ_2 and/or ζ_3 does bring the system closer to the Coulomb interaction region, which suggests that Modes 2 and 3 must be anharmonic.

In the numerical calculations the size of the Gaussian quadrature was $M_1 = M_2 = M_2 = 21$ and the basis set size was $N_1 \times N_2 \times N_3 = 15 \times 15 \times 15$. With these parameters the accuracy of lowest 420 states was better than 10^{-9} MHz. Table 3 gives several eigenvalues computed numerically, their assignments and deviations δE from the harmonic model, Eq. (39). Figure 6 shows the deviations δE for the three normal mode progressions. From these data we see that Mode 1 is indeed harmonic in agreement with the arguments given above, while Modes 2 and 3 are slightly anharmonic, due to Coulomb interaction. Frequencies and anharmonicity coefficients for the Dunham expansion are given in Table 4. We see that in this case $\Delta_2 \sim 10^{-6}\omega_2$ and $\Delta_3 \sim 10^{-5}\omega_3$, which means that the asymmetric stretching mode is more anharmonic (by about

an order of magnitude) than the symmetric stretching mode. Still this anharmonicity (due to Coulomb) is very low and is insufficient for the control.

We had an intuitive feeling that the Coulomb anharmonicity could, probably, be increased by bringing the ions closer together, which can be achieved by raising the force constant k (*i.e.*, by making the trapping potential sharper). In order to test this hypothesis we carried out a set of calculations with different values of k. In the most dramatic case we raised k by a factor of $\alpha = 50$. Results are collected in three frames of Fig. 7. Figure 7(a) gives frequencies of three normal modes *vs.* equilibrium distances between ions. Figures 7(b) and 7(c) give the intra- and inter-mode anharmonicity parameters *vs.* frequency. From these pictures we see that amount of Coulomb anharmonicity (expressed through anharmonicity parameters) increases as we bring the ions closer together (by raising the value of k). However, this increase is not substantial (roughly linear) and occurs simultaneously with very fast increase of the frequencies. For example, when the value of k is raised by a factor of $\alpha = 50$, the value of $z_3^{eq} \approx 2500\, a_0$ is observed and the values of frequencies are roughly a factor of seven larger compared to the original case ($\alpha = 1$). The values of $\Delta_1/2\pi$ stay zero independently of k, while values of $\Delta_2/2\pi$, $\Delta_3/2\pi$ and $\Delta_{23}/2\pi$ all increase. The values of $\Delta_3/2\pi$ and $\Delta_{23}/2\pi$ increase faster (compared to that of $\Delta_2/2\pi$) and reach roughly -1.9×10^{-4} MHz when the frequency reaches $\omega_3/2\pi \approx 47$ MHz. As a result, we still have $\Delta_3 \sim 10^{-5}\,\omega_3$.

In conclusion, the three-ion system in the harmonic trap shows some minor anharmonicity of two stretching modes, due to the Coulomb interaction. The amount of this anharmonicity is, however, insufficient for the control. The center-of-mass motion mode is exactly harmonic. Modifying the trapping potential is essential for achieving higher levels anharmonicity, which was attempted next.

4.b. Strongly Anharmonic Trap

To represent the case of a strongly anharmonic trap we used the potential proportional to z^4. The trap component of the 3D-PES in Eq. (31) was:

$$V_{\text{trap}}(z_1, z_2, z_3) = k' \frac{z_1^4}{4!} + k' \frac{z_2^4}{4!} + k' \frac{z_3^4}{4!}. \tag{44}$$

The value of $k'/2\pi = 1.494 \times 10^{-7}$ MHz/a_0^4 was chosen in order to obtain the inter-nuclear distances similar to those in the harmonic trap studied above (with the purpose to have similar magnitude of the Coulomb anharmonicity). Numerical minimization in this potential gave $z_1^{eq} = -2.209 \times 10^3$ a_0, $z_2^{eq} \approx 0$, and $z_3^{eq} = 2.209 \times 10^3$ a_0. Energy at the minimum was $V^{eq}/2\pi = V(z_1^{eq}, z_2^{eq}, z_3^{eq})/2\pi = 1.482 \times 10^6$ MHz. Diagonalization of the Hessian matrix gave $\omega_1/2\pi = 31.03$ MHz, $\omega_2/2\pi = 56.07$ MHz and $\omega_3/2\pi = 62.78$ MHz. The eigenvectors of the three corresponding modes were:

$$\mathbf{A} = \begin{vmatrix} 0.4197 & 0.7071 & -0.5691 \\ 0.8048 & 0.0000 & 0.5935 \\ 0.4197 & -0.7071 & -0.5691 \end{vmatrix}. \tag{45}$$

The Hamiltonian was transformed into the normal mode coordinates using these eigenvectors; the PES transformed into these coordinates is shown in Fig. 8. From a brief glance at this picture it becomes apparent that all three modes are anharmonic. The motion from the minimum energy point along any axis (ζ_1, ζ_2 or ζ_3) brings the system closer to the white part of the picture (strong Coulomb repulsion) and results in appearance of the Coulomb anharmonicity.

Note that the Modes 1 and 3 of the anharmonic trap, Eq. (45), are different from those of the Harmonic trap, Eq. (42). We see that in Eq. (45) $a_{21} > a_{11} = a_{31}$ and $|a_{23}| > |a_{13}| = |a_{33}|$. This

happens because the $\sim z^4$ potential is flatter in the center and is sharper near the turning points, compared to the harmonic case. As a result, the amplitude of motion of the central ion is larger than the amplitudes of motion of the terminal ions. We found that in such normal mode coordinates the potential coupling terms do not cancel and the three-dimensional Hamiltonian is non-separable. All three degrees of freedom are coupled and this case must be treated numerically.

In numeric calculations the size of the Gaussian quadrature was $M_1 = M_2 = M_2 = 21$ and the basis set size was $N_1 \times N_2 \times N_3 = 15 \times 15 \times 15$. This provided accuracy better than 10^{-9} MHz to the lower 250 vibrational states. The spectrum of states is given in Table 5. Deviations of the normal mode progressions from the harmonic model are presented in Fig. 9. Figure 9 shows very clearly that in the anharmonic trap all three normal modes are slightly anharmonic (contrast to Fig. 6). Anharmonicities of the Modes 1 and 2 are very similar. Mode 3 is the most anharmonic mode.

Unfortunately, we found that the absolute values of these anharmonicities are quite low. Coefficients of the fit by the Dunham expansion are given in Table 6. These data show that for the most anharmonic Mode 3 (asymmetric stretching mode) the parameter of anharmonicity reaches only $\Delta_3 \sim 10^{-5}\omega_3$, insufficient for the control. This means that a strongly anharmonic trap offers no improvements over the purely harmonic trap.

It was quite surprising to find that the spectrum of three ions in a *highly* anharmonic trap is only *slightly* anharmonic. It was especially unexpected to see that the center-of-mass motion mode (Mode 1) is the less anharmonic mode. Based on general arguments one might expect that the center-of-mass motion mode of three ions in an anharmonic trap describes the motion similar to vibration of one ion in an anharmonic trap. Since anharmonicity of the one-ion spectrum was

very pronounced (see Sec. 2), we expected to see the effect of similar magnitude in the three-ion case. It appears, however, that the Mode 1 in an anharmonic trap is special; it is different from the center-of-mass mode in the harmonic trap. Namely, in the anharmonic potential the terminal ions are allowed to move less than the central atom (see Eq. (45)), which compensates for anharmonicity of the trapping potential and makes the Mode 1 less anharmonic. Put another way, for Mode 1 in the anharmonic trap the arrangement of three ions is not rigid and adjusts to the changes of the potential, minimizing the effect of anharmonicity. The positive outcome of this effect is that all three modes become anharmonic. The negative outcome is that the values of anharmonicity parameters remain small.

We hoped to increase the values of anharmonicity parameters in this system by raising the value of force constant k'. A number of computational experiments were carried out. Their results are presented in Fig. 10. As one might expect, the frequencies of three vibrational modes increase as k' is raised, while the eqilibrium internuclear distances decrease (see Fig. 10(a)). Frequenicies of Modes 2 and 3 remain close to each other and are about twice higher than the frequency of Mode 1. As k' is raised all three intramode anharmonicity parameters (see Fig. 10(b)) and all three intermode anharmonicity parameters (see Fig. 10(c)) grow about linearly. The Mode 3 remains most anharmonic. When k' is raised by a factor of $\beta = 525$, anharmonicity of this mode reaches almost $\Delta_3/2\pi$ = –6.4×10^{-4} MHz. However, the frequency of this mode grows at the same time and reaches almost $\omega_3/2\pi$ = 64 MHz, leading to about the same relative effect of anharmonicity: $\Delta_3 \sim 10^{-5}\omega_3$. Indeed, the linear dependencies in Figs. 10(b, c) here and in Figs. 7(b, c) above demonstrate very clearly that raising force constant has negligible effect on the Δ_i / ω_i ratios in both harmonic and strongly anharmonic traps.

We also experimented with combinations of the harmonic and anharmonic terms in the trapping potential $V_{\text{trap}}(z) = \alpha k z^2/2 + \beta k' z^4/4!$ where both α and β were positive numbers. In this way we studied a large number of anharmonic traps with various α-to-β ratios, from slightly anharmonic to strongly anharmonic. We did not find any useful combination.

In conclusion, we showed that the vibrational spectrum of three ions in the usual trap architectures (either purely harmonic, slightly anharmonic or strongly anharmonic) exhibits only minor anharmonicity. Motional states of ions in such traps cannot be efficiently controlled using approach of Ref. [1].

4.c. Inverted Combined Trap

Here we considered a trapping potential of the form:

$$V_{\text{trap}}(z) = \alpha k \frac{z^2}{2} + \beta k' \frac{z^4}{4!}, \tag{46}$$

where β is positive but α is a *negative* number. When the $-\alpha/\beta$ ratio is very large this expression describes a double well potential with two (separated, almost independent) wells, but we are far from that limit. In the cases considered here the first term of Eq. (46) lifts, just slightly, the potential in the middle of the z^4 well, creating a wide, strongly anharmonic trap [18], with the vibrational zero-point energy well above the top of the barrier at $z = 0$.

The values of force parameters k and k' here were equal to those before. The values of α and β were varied. In the discussion that follows we present a series of calculations with α = -100 and β = 1, 1.05, 1.10, 1.14, 1.19 and 1.43. Consider the case of $\beta = 1$. Numerical minimization gave $z_1^{eq} = -2.862\times10^3\, a_0$, $z_2^{eq} \approx 0$ and $z_3^{eq} = 2.862\times10^3\, a_0$. Energy at this point was $V^{eq}/2\pi = V(z_1^{eq}, z_2^{eq}, z_3^{eq})/2\pi = 5.359\times10^5$ MHz. The normal mode frequencies were

$\omega_1/2\pi = 2.734$ MHz, $\omega_2/2\pi = 54.58$ MHz and $\omega_3/2\pi = 54.89$ MHz. Their corresponding eigenvectors were:

$$\mathbf{A} = \begin{vmatrix} 0.1578 & 0.7071 & -0.6893 \\ 0.9748 & 0.0000 & 0.2231 \\ 0.1578 & -0.7071 & -0.6893 \end{vmatrix}. \quad (47)$$

Note that two frequencies in this system are very close and are much higher than the third frequency: $\omega_1 << \omega_2 \sim \omega_3$. The normal Modes 1 and 3 are very unusual. Mode 1 describes motion where amplitude of the central ion is almost an order of magnitude larger than amplitudes of the terminal ions: $a_{21} >> a_{11} = a_{31}$. Mode 3 shows just opposite: $|a_{23}| << |a_{13}| = |a_{33}|$. The PES of this system, transformed into the normal mode coordinates of Eq. (47), is shown in Fig. 11. From analysis of Fig. 11 one can expect that in this system Mode 1 is the most anharmonic. Somewhat less obvious but still possible to derive from Fig. 11 is that the Modes 2 and 3 are also somewhat anharmonic, because the motion along ζ_2 and ζ_3 axes brings the system closer to the highly repulsive (white) area of the PES.

The behavior of Mode 1 is easy to explain. The central atom sits on the top of a small "hill" so that its deviation from the equilibrium point reduces the potential energy, compensating for increase of potential energy due to the motion of terminal atoms. As a result, the PES is very flat along ζ_1 and is very anharmonic. The behavior of Mode 3 is less intuitive, or even somewhat counterintuitive. We think that the Mode 3 is as it is simply because it must be orthogonal to the Modes 1 and 2. Overall, the Mode 1 (low frequency mode) describes mostly the motion of central ion, while the Modes 2 and 3 (high frequency, nearly degenerate modes) describe mostly the motion of two terminal ions.

In numerical calculations, due to very different frequencies of the modes, we used the following parameters: $M_1 = 21$, $M_2 = M_3 = 17$ for the Gaussian quadratures in ζ_1, ζ_2 and ζ_3, respectively, and $N_1 \times N_2 \times N_3 = 15 \times 10 \times 10$ for the basis set size. Accuracy was comparable to or better than in the calculations presented above (10^{-9} MHz to the lower 364 vibrational states). The spectrum of numerical eigenvalues is given in Table 7, along with the state assignments and deviations of their energies from the analytic harmonic model. Figure 12 shows deviations from the harmonic model for the three normal mode progressions. From this picture we see that all three normal modes are strongly anharmonic, with the Mode 1 being the most anharmonic. Anharmonicities of the Modes 2 and 3 seem to be comparable. Coefficients of the Dunham expansion fit for this spectrum were computed and presented in Table 8. Anharmonicity parameters in this system show dramatic improvement compared to all cases studied above. We see that $\Delta_1 \sim 10^{-2}\omega_1$, which is well sufficient for the successful control. Mode 3 is less anharmonic, $\Delta_3 \sim 10^{-4}\omega_3$, but it is still more anharmonic than any mode in the $\sim z^4$ potential studied above.

Variations of the $-\alpha/\beta$ ratio reveal an important and interesting property of this system. When β is raised (from $\beta = 1$ to $\beta = 1.43$ in Fig. 13) the frequencies of all modes increase (see Fig. 13(a, b)) while the values of anharmonicity parameters all drop (see Fig. 13(c-f)). This behavior is exactly opposite to that seen in the $\sim z^2$ and $\sim z^4$ traps studied above. It appears that in the case of inverted combined potential there is no reason to raise β. When $\alpha = -100$, small values of $\beta \le 1$ are appropriate. The dependence of anharmonicity *vs.* frequency in Fig. 13 is quite dramatic. Note that the case we presented here in detail ($\alpha = -100$, $\beta = 1$) is, in fact, just on the edge of the region where anharmonicity increases very sharply. If

we move further into the region of small β or, alternatively, increase the value of α, even more anharmonic system is obtained. We conclude that the low frequency/high anharmonicity system can be readily created by the appropriate choice of the two force constants in the inverted combined potential of Eq. (46).

Using accurate energies and wave functions obtained here we computed the transition moment matrix numerically (for the $\alpha = -100$, $\beta = 1$ case) and carried out the OCT calculations of the major one-qubit gates (NOT, Hadamard transform, etc) and some two-qubit gates (such as CNOT) in this system. The control qubit was encoded into the $|v=0\rangle$ and $|v=1\rangle$ states of the less anharmonic Mode 3. Second qubit was encoded into the $|v=0\rangle$ and $|v=1\rangle$ states of the most anharmonic Mode 1. Results of these calculations are very optimistic. They will be reported in the second paper of this series (Paper II) in the near future.

5. Conclusions

In this paper we presented a general numerical approach to accurate theoretical studies of the vibrational spectra of ions in a trap. We applied this method to study one, two, and three ions in several different trapping potentials. For one ion in a slightly anharmonic trap we were able to confirm all conclusions of Ref. [1] concerning the new scheme of adiabatic and coherent control based on selective excitation of the vibrational states by optimally shaped pulses. By the OCT calculations we confirmed that anharmonicity of the vibrational spectrum on the order of 1% of the frequency, $\Delta \sim 10^{-2}\omega$, is sufficient for successful accurate control.

For two ions in a harmonic trap we reached the level of accuracy that allowed us to quantify the anharmonic effect of Coulomb interaction, $\Delta \sim 10^{-5}\omega$. We believe that Coulomb anharmonicity in the ion trap has been accessed and characterized theoretically for the first time.

To our best knowledge in all previous studies the Coulomb anharmonicity has been neglected (as we discussed earlier in the harmonic approximation presented here). By studying two ions in a trap we also found that the symmetric stretching mode is dark and cannot be controlled. This conclusion is valid not just for two, but also for three and more trapped ions.

For three ions in a harmonic trap we characterized the magnitude of Coulomb anharmonicity and concluded that it is insufficient for selective control of the vibrational motion, $\Delta \sim 10^{-5}\omega$. We also studied the system of three ions in a strongly anharmonic trap but found that it does not offer any advantages. Vibrational anharmonicities remain low due to special properties of the normal vibration modes: The center-of-mass motion of three ions is such that the anharmonic effect of the trapping potential is minimized and the system finds the less anharmonic path on the PES. All three modes in such systems are coupled and are somewhat anharmonic, but the amount of anharmonicity is insufficient for the control, $\Delta \sim 10^{-5}\omega$.

The most practically important results of this work belong to the system of three ions in an inverted combined potential trap. We found that this system has a number of favorable properties. First of all, the lowest frequency mode (the center-of-mass motion mode) is also the most anharmonic, which provides $\Delta \sim 10^{-2}\omega$, well sufficient for the successful control. Although the other two modes are nearly degenerate, one of them is dark (symmetric stretching) and should not interfere with selective excitation of the active mode (asymmetric stretching). Anharmonicity of the asymmetric stretching mode is smaller, $\Delta \sim 10^{-4}\omega$, but this mode is anharmonic enough to serve for encoding the *control* qubit. Finally, frequencies of the two controllable modes (center-of-mass and the asymmetric stretching) are very different, which is quite useful for selective addressing of the two modes in the experiment. Large separation of

frequencies of these modes should also provide good coherence properties of two independent qubits encoded into these modes.

The dependence of anharmonicity *vs.* frequency in the inverted combined potential is favorable and allows reaching a high degree of anharmonicity without raising the frequency. This property suggests that the suitable set of parameters we found and used in this work is not unique. By varying the values of two force constants in the inverted combined potential one can create a system with desirable properties. This suggests favorable applications to future experiments.

ACKNOWLEDGEMENTS

This work was supported by the National Science Foundation, grant number CHE-1012075. This research used resources of the National Energy Research Scientific Computing Center, which is supported by the Office of Science of the U.S. Department of Energy under Contract No. DE-AC02-05CH11231. Professor Martine Gruebele at the University of Illinois at Urbana-Champaign is acknowledged for fruitful discussions.

References

[1] M. Zhao and D. Babikov, Phys. Rev. A **77**, 012338 (2008).

[2] J. I. Cirac and P. Zoller, Phys. Rev. Lett. **74**, 4091 (1995).

[3] C. Monroe, D. M. Meekhof, B. E. King, W. M. Itano, and D. J. Wineland, Phys. Rev. Lett. **75**, 4714 (1995).

[4] D. M. Meekhof, C. Monroe, B. E. King, W. M. Itano, and D. J. Wineland, Phys. Rev. Lett. **76**, 1796 (1996).

[5] C. A. Sackett D. Keilpinski, B. E. King, C. Langer, V. Meyer, C. J. Myatt, M. Rowe, A. A. Turchette, W. M. Itano, D. J. Wineland, and C. Monroe, Nature (London) **404**, 256 (2000).

[6] J. J. Garcia-Ripoll, P. Zoller, and J. I. Cirac., Phys. Rev. Lett. **91**, 157901 (2003).

[7] F. Schmidt-Kaler, H. Haeffner, R. Riebe, S. Gulde, G. P. T. Lancaster, T. Deuschle, C. Becher, C. F. Roos, J. Eschner, and R. Blatt, Nature (London) **422**, 408 (2003).

[8] H. Haeffner, W. Haensel, C. F. Roos, J. Benhelm, D. Chek-alkar, M. Challa, T. K. Farber, U. D. Rapol, M. Riebe, P. O. Schmidt, C. Becher, O. Gahne, and D. J. Wineland, Nature (London) **438**, 643 (2005).

[9] D. Leibfried *et al.*, Nature (London) **438**, 639 (2005).

[10] F. Schmidt-Kaler, H. Häffner, S. Gulde, M. Riebe, G. P.T. Lancaster, T. Deuschle, C. Becher, W. Hänsel, J. Eschner, C. F. Roos, and R. Blatt, Appl. Phys. B **77**, 789 (2003).

[11] P. Bushev, D. Rotter, A. Wilson, F. Dubin, C. Becher, J. Eschner, R. Blatt, V. Steixner, P. Rabl, and P. Zoller, Phys. Rev. Lett. **96**, 043003 (2006).

[12] C. Monroe and D. Wineland, Scientific American (August, 2008), pp. 64-71.

[13] D. Leibfried, R. Blatt, C. Monroe, and D. Wineland, Rev. Mod. Phys. **75**, 281 (2003).

[14] R. Blatt and D. J. Wineland, Nature 453, 1008 (2008).

[15] K. Kim, M.-S. Chang, R. Islam, S. Korenblit, L.-M. Duan, and C. Monroe, Phys. Rev. Lett. **103**, 120502 (2009).

[16] K. Kim, M.-S. Chang, S. Korenblit, R. Islam, E. E. Edwards, J. K. Freericks, G.-D. Lin, L.-M. Duan, and C. Monroe, Nature **465**, 590 (2010).

[17] L.-M. Duan and C. Monroe, Rev. Mod. Phys. **82**, 1209 (2010).

[18] G. D. Lin, S. L. Zhu, R. Islam, K. Kim, M. S. Chang, S. Korenblit, C. Monroe, and L. M. Duan, Europhysics. Lett. **86**, 60004, (2009).

[19] D. Babikov, J. Chem. Phys. **121**, 7577 (2004).

[20] M. Zhao and D. Babikov, J. Chem. Phys. **126**, 204102 (2007).

[21] Y. Y. Gu and D. Babikov, J. Chem. Phys. **131**, 034306 (2009).

[22] C. Gollub, U. Troppmann, and R. De Vivie-Riedle, New J. Phys. **8**, 48 (2006).

[23] L. Wang and D. Babikov, *"Adibatic coherent control in the anharmonic ion trap: II. Optimal control studies of quantum gates"*, unpublished.

[24] B. B. Blinov, D. L. Moehring, L.-M. Duan, and C. Monroe, Nature **428**, 153 (2004).

[25] L. Deslauriers, S. Olmschenk, D. Stick, W. K. Hensinger, J.Sterk, and C. Monroe, Phys. Rev. Lett. **97**, 103007 (2006).

[26] L. Deslauriers *et al.*, Phys. Rev. A **74**, 063421 (2006).

[27] B. H. Bransden and C. J. Joachain , Introduction to Quantum Mechanics. (1989).

[28] DSYEV from LAPACK is a software package provided by Univ. of Tennessee, Univ. of California Berkeley, Univ. of Colorado Denver and NAG Ltd, (2006).
[29] National Energy Research Scientific Computing Center (www.nersc.gov).
[30] W. Demtröder, Molecular Physics. (2005)
[31] A. R. Leach, Molecular Modelling-Principles and Applications (Second edition). (2001).
[32] F. Jensen, Introduction to Computational Chemistry. (1999).
[33] T. P. Meyrath and D. F. V. James, Phys. Lett. A. **240**, 37, (1998).
[34] D. F. V. James, Appl. Phys. B. **66**, 181, (1998).
[35] D.J. Wineland, C. Monroe, W.M. Itano, D. Leibfried, B. King, and D.M. Meekhof, Journal of Research of the National Institute of Standards and Technology **103**, 259 (1998).
[36] W. H. Press, S. A. Teukolsky, W. T. Vetterling, and B. P. Flannery, Numerical Recipes (Third edition). (2007).
[37] www.mhpcc.edu/training/workshop/mpi/MAIN.html. (2003).

State #	$E/2\pi$ (MHz)	v	$\delta E/2\pi$ (MHz)
1	1.3964	0	0.0114
2	4.2115	1	0.0565
3	7.0702	2	0.1452
4	9.9707	3	0.2758
5	12.9115	4	0.4465
6	15.8910	5	0.6560
7	18.9079	6	0.9029
8	21.9611	7	1.1861
9	25.0494	8	1.5044
10	28.1718	9	1.8568
11	31.3273	10	2.2423

Table 1: Eigenvalues, assignments and deviations (from the harmonic model) of the vibrational states of one ion in a slightly anharmonic trap.

State #	$E/2\pi$ (MHz)	(v_1, v_2)	$\delta E/2\pi$ (10^{-4} MHz)
1	3.7839	(0, 0)	0.0785
2	6.5539	(1, 0)	0.0777
3	8.5817	(0, 1)	0.2135
4	9.3239	(2, 0)	0.0768
5	11.3517	(1, 1)	0.2127
6	12.0939	(3, 0)	0.0760
7	13.3795	(0, 2)	0.4856
8	14.1217	(2, 1)	0.2119
9	14.8639	(4, 0)	0.0752
10	16.1495	(1, 2)	0.4848
11	16.8917	(3, 1)	0.2110
12	17.6339	(5, 0)	0.0743
13	18.1773	(0, 3)	0.8947
14	18.9195	(2, 2)	0.4839
15	19.6617	(4, 1)	0.2102
16	20.4039	(6, 0)	0.0735
17	20.9473	(1, 3)	0.8938
18	21.6895	(3, 2)	0.4831
19	22.4317	(5, 1)	0.2093
20	22.9751	(0, 4)	1.4407
21	23.1739	(7, 0)	0.0726
26	25.9439	(8, 0)	0.0718
29	27.7730	(0, 5)	2.1238
40	32.5709	(0, 6)	2.9439
53	37.3687	(0, 7)	3.9010
67	42.1666	(0, 8)	4.9951

Table 2: Eigenvalues, assignments and deviations (from the harmonic model) of the vibrational states of two ions in a harmonic trap.

State #	$E/2\pi$ (MHz)	(v_1, v_2, v_3)	$\delta E/2\pi$ (10^{-3} MHz)
1	7.1194	(0, 0, 0)	0.0243
2	9.8894	(1, 0, 0)	0.0243
3	11.9172	(0, 1, 0)	0.0364
4	12.6594	(2, 0, 0)	0.0243
5	13.7905	(0, 0, 1)	0.0583
6	14.6872	(1, 1, 0)	0.0364
7	15.4294	(3, 0, 0)	0.0255
8	16.5605	(1, 0, 1)	0.0595
9	16.7150	(0, 2, 0)	0.0522
10	17.4572	(2, 1, 0)	0.0364
11	18.1994	(4, 0, 0)	0.0243
12	18.5883	(0, 1, 1)	0.0838
13	19.3305	(2, 0, 1)	0.0583
14	19.4850	(1, 2, 0)	0.0522
15	20.2272	(3, 1, 0)	0.0364
16	20.4616	(0, 0, 2)	0.1214
17	20.9694	(5, 0, 0)	0.0243
18	21.3583	(1, 1, 1)	0.0850
19	21.5128	(0, 3, 0)	0.0729
20	22.1005	(3, 0, 1)	0.0583
25	23.7394	(6, 0, 0)	0.0243
34	26.3106	(0, 4, 0)	0.0996
35	26.5094	(7, 0, 0)	0.0243
38	27.1327	(0, 0, 3)	0.2089
47	29.2794	(8, 0, 0)	0.0243
56	31.1084	(0, 5, 0)	0.1287
72	33.8039	(0, 0, 4)	0.3230
86	35.9062	(0, 6, 0)	0.1651
124	40.4751	(0, 0, 5)	0.4663
126	40.7041	(0, 7, 0)	0.2040
176	45.5019	(0, 8, 0)	0.2477
196	47.1463	(0, 0, 6)	0.6363
289	53.8175	(0, 0, 7)	0.8306
403	60.4888	(0, 0, 8)	1.0491

Table 3: Eigenvalues, assignments and deviations (from the harmonic model) of the vibrational states of three ions in a harmonic trap.

Mode frequency $\omega_i/2\pi$ (MHz), i=1, 2, 3	Intramode anharmonicity $\Delta_i/2\pi$ (MHz), i=1, 2, 3	Intermode anharmonicity $\Delta_{ij}/2\pi$ (MHz)
2.770	~ 0	$\Delta_{12} \sim 0$
4.798	-2.343×10^{-6}	$\Delta_{13} \sim 0$
6.671	-1.358×10^{-5}	$\Delta_{23}/2\pi = -1.393\times10^{-5}$

Table 4: Coefficients of the fit by the Dunham expansion formula, Eq. (40), of the numerically calculated spectrum in Table 3 (vibrational states in the harmonic trap). The shift parameter was $D/2\pi = -1.757\times10^{-5}$ MHz.

State #	$E/2\pi$ (MHz)	(v_1, v_2, v_3)	$\delta E/2\pi$ (10^{-2} MHz)
1	74.9440	(0, 0, 0)	0.1054
2	105.9766	(1, 0, 0)	0.1778
3	131.0160	(0, 1, 0)	0.1778
4	137.0095	(2, 0, 0)	0.2827
5	137.7282	(0, 0, 1)	0.2691
6	162.0489	(1, 1, 0)	0.2788
7	168.0428	(3, 0, 0)	0.4216
8	168.7613	(1, 0, 1)	0.3905
9	187.0885	(0, 2, 0)	0.2875
10	193.0822	(2, 1, 0)	0.4119
11	193.8006	(0, 1, 1)	0.3769
12	199.0764	(4, 0, 0)	0.5926
13	199.7947	(2, 0, 1)	0.5440
14	200.5137	(0, 0, 2)	0.5556
15	218.1217	(1, 2, 0)	0.4177
16	224.1157	(3, 1, 0)	0.5790
17	224.8340	(1, 1, 1)	0.5265
18	230.1104	(5, 0, 0)	0.8004
19	230.8285	(3, 0, 1)	0.7324
20	231.5472	(1, 0, 2)	0.7247
21	243.1613	(0, 3, 0)	0.4391
22	249.1552	(2, 2, 0)	0.5809
23	249.8734	(0, 2, 1)	0.5226
24	255.1496	(4, 1, 0)	0.7830
25	255.8677	(2, 1, 1)	0.7091
26	256.5864	(0, 1, 2)	0.6975
27	261.1446	(6, 0, 0)	1.0394
28	261.8626	(4, 0, 1)	0.9520
29	262.5812	(2, 0, 2)	0.9267
30	263.3003	(0, 0, 3)	0.9617
31	274.1948	(1, 3, 0)	0.5984
32	280.1891	(3, 2, 0)	0.7810
33	280.9071	(1, 2, 1)	0.7014
34	286.1839	(5, 1, 0)	1.0180
41	299.2346	(0, 4, 0)	0.6295
55	326.0882	(0, 0, 4)	1.4921
68	355.3082	(0, 5, 0)	0.8626
92	388.8773	(0, 0, 5)	2.1449
104	411.3823	(0, 6, 0)	1.1346
148	451.6677	(0, 0, 6)	2.9181

Table 5: Eigenvalues, assignments and deviations (from the harmonic model) of the vibrational states of three ions in a strongly anharmonic trap.

Mode frequency $\omega_i/2\pi$ (MHz), i=1, 2, 3	Intramode anharmonicity $\Delta_i/2\pi$ (MHz), i=1, 2, 3	Intermode anharmonicity $\Delta_{ij}/2\pi$ (MHz)
31.032	-1.667×10^{-4}	$\Delta_{12}/2\pi = -2.916\times10^{-4}$
56.071	-1.989×10^{-4}	$\Delta_{13}/2\pi = -4.859\times10^{-4}$
62.783	-6.103×10^{-4}	$\Delta_{23}/2\pi = -3.517\times10^{-4}$

Table 6: Coefficients of the fit by the Dunham expansion formula, Eq. (40), of the numerically calculated spectrum in Table 5 (vibtational states in the strongly anharmonic trap). The shift parameter was $D/2\pi = -5.269\times10^{-4}$ MHz.

State #	$E/2\pi$ (MHz)	(v_1, v_2, v_3)	$\delta E/2\pi$ (MHz)
1	56.1289	(0, 0, 0)	0.0271
2	58.9625	(1, 0, 0)	0.1264
3	61.8832	(2, 0, 0)	0.3130
4	64.8846	(3, 0, 0)	0.5802
5	67.9611	(4, 0, 0)	0.9225
6	71.1081	(5, 0, 0)	1.3354
7	74.3218	(6, 0, 0)	1.8149
16	110.6932	(0, 1, 0)	0.0122
17	111.0009	(0, 0, 1)	0.0089
46	165.2552	(0, 2, 0)	-0.0049
48	165.8757	(0, 0, 2)	-0.0065
89	219.8143	(0, 3, 0)	-0.0251
94	220.7524	(0, 0, 3)	-0.0201
149	274.3688	(0, 4, 0)	-0.0498
153	275.6304	(0, 0, 4)	-0.0323
222	328.9163	(0, 5, 0)	-0.0815
229	330.5096	(0, 0, 5)	-0.0434
311	383.4522	(0, 6, 0)	-0.1248
318	385.3897	(0, 0, 6)	-0.0535

Table 7: Eigenvalues, assignments and deviations (from the harmonic model) of the vibrational states of three ions in a combined inverted trap with $\alpha = -100$ and $\beta = 1$. See text for details.

Mode frequency $\omega_i/2\pi$ (MHz), i=1, 2, 3	Intramode anharmonicity $\Delta_i/2\pi$ (MHz), i=1, 2, 3	Intermode anharmonicity $\Delta_{ij}/2\pi$ (MHz)
2.738	-4.361×10^{-2}	$\Delta_{12}/2\pi = -1.102\times10^{-2}$
54.580	1.106×10^{-3}	$\Delta_{13}/2\pi = -4.871\times10^{-3}$
54.886	-1.371×10^{-3}	$\Delta_{23}/2\pi = 3.872\times10^{-2}$

Table 8: Coefficients of the fit by the Dunham expansion formula, Eq. (40), of the numerically calculated spectrum in Table 7 (vibtational states in the combined inverted trap). The shift parameter was $D/2\pi = -2.115\times10^{-2}$ MHz.

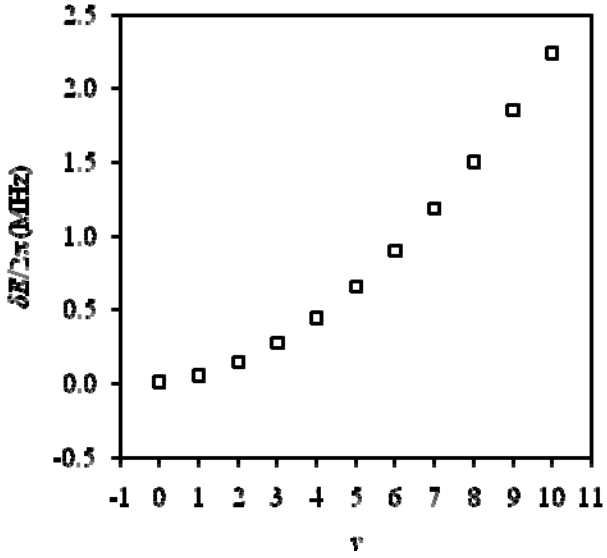

Fig. 1: Effect of anharmonicity on the vibrational spectrum of one ion in a slightly anharmonic potential trap.

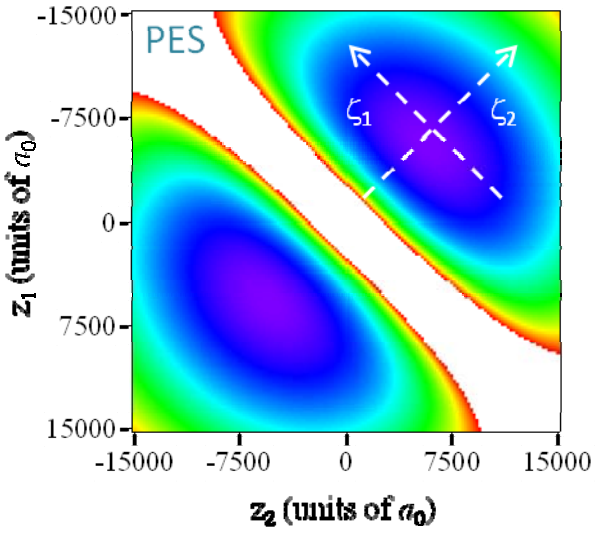

Fig. 2: Potential energy surface of two ions in the harmonic potential trap. Anharmonicities due to Coulomb repulsion of ions are clearly seen.

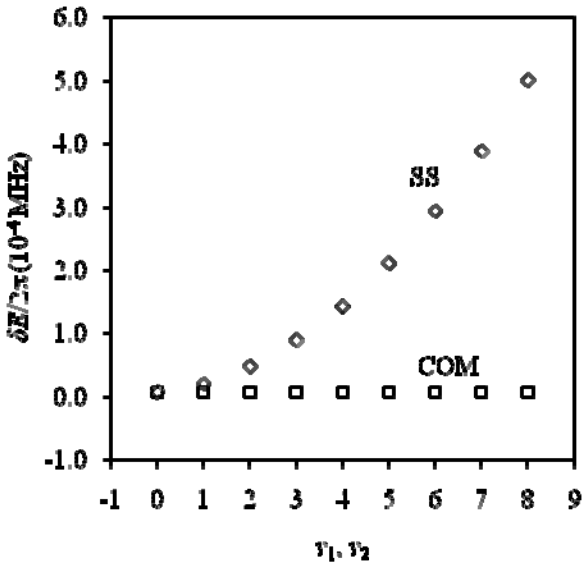

Fig. 3: Effect of anharmonicity on two modes of the vibrational spectrum of two ions in a harmonic ($\sim z^2$) potential trap -- the center-of-mass motion (COM) mode and the symmetric stretching (SS) mode.

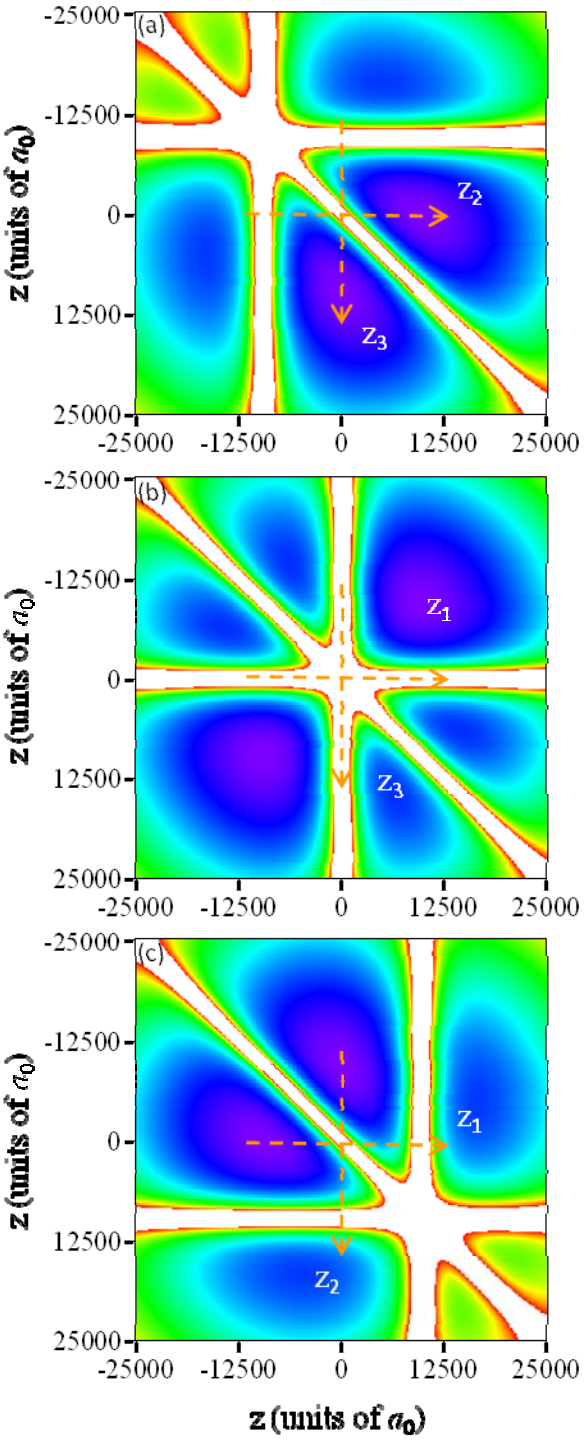

Fig. 4: Potential energy surface of three ions in the harmonic potential trap using Cartesian coordinates. Three slices through the 3D-surface are shown: *a*) perpendicular to z_1 through $z_1 = 0$, *b*) perpendicular to z_2 through $z_2 = 0$ and *c*) perpendicular to z_3 through $z_3 = 0$.

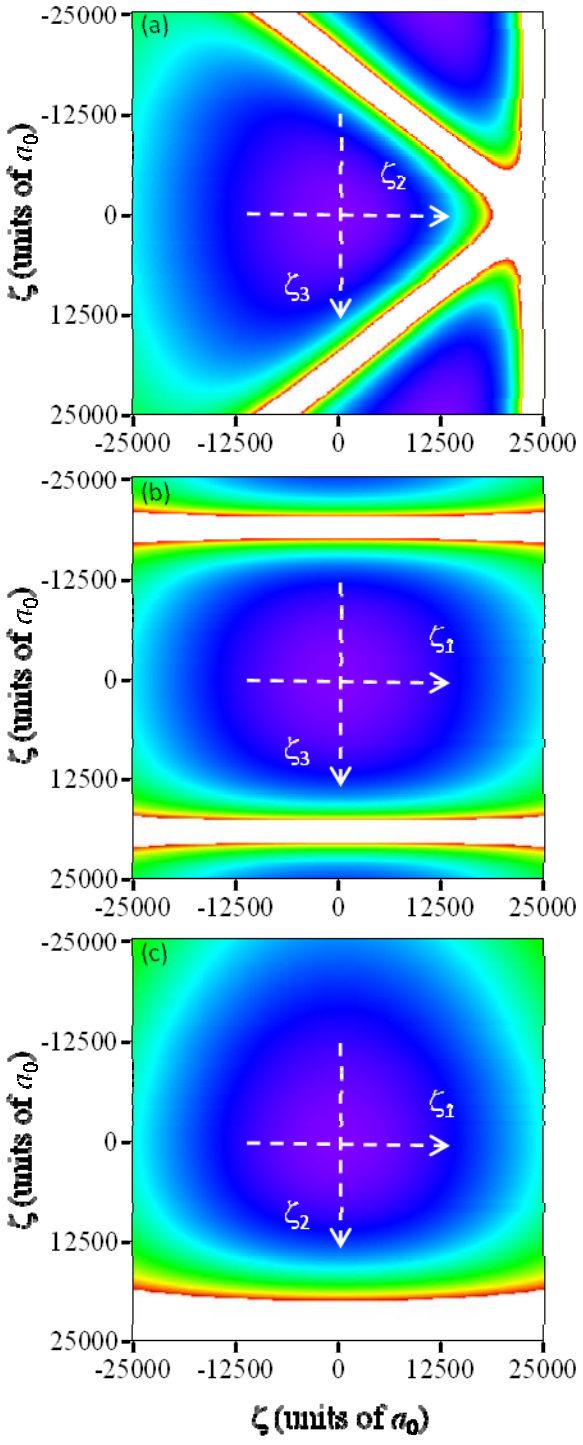

Fig. 5: Potential energy surface of three ions in the harmonic potential trap using the normal mode coordinates. Three slices through the 3D-surface are shown: *a*) perpendicular to ζ_1 through $\zeta_1 = 0$, *b*) perpendicular to ζ_2 through $\zeta_2 = 0$ and *c*) perpendicular to ζ_3 through $\zeta_3 = 0$. Note that the Coulomb repulsion part (white) goes parallel to ζ_1 everywhere.

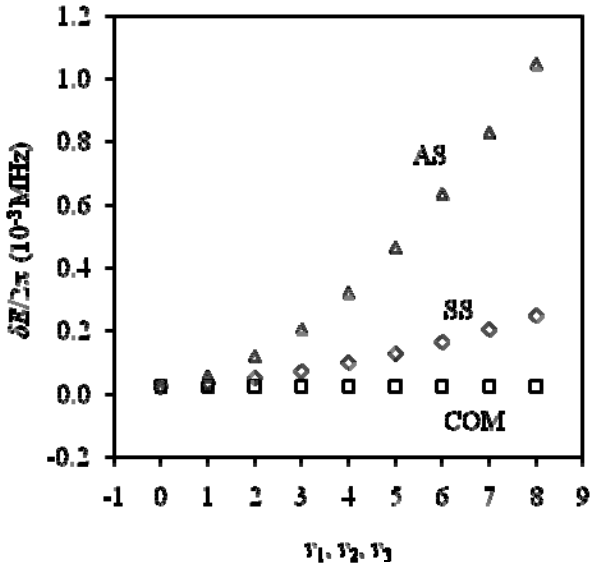

Fig. 6: Effect of anharmonicity on three modes of the vibrational spectrum of three ions in a harmonic ($\sim z^2$) potential trap -- the center-of-mass motion (COM) mode, the symmetric stretching (SS) mode and the asymmetric stretching (AS) mode.

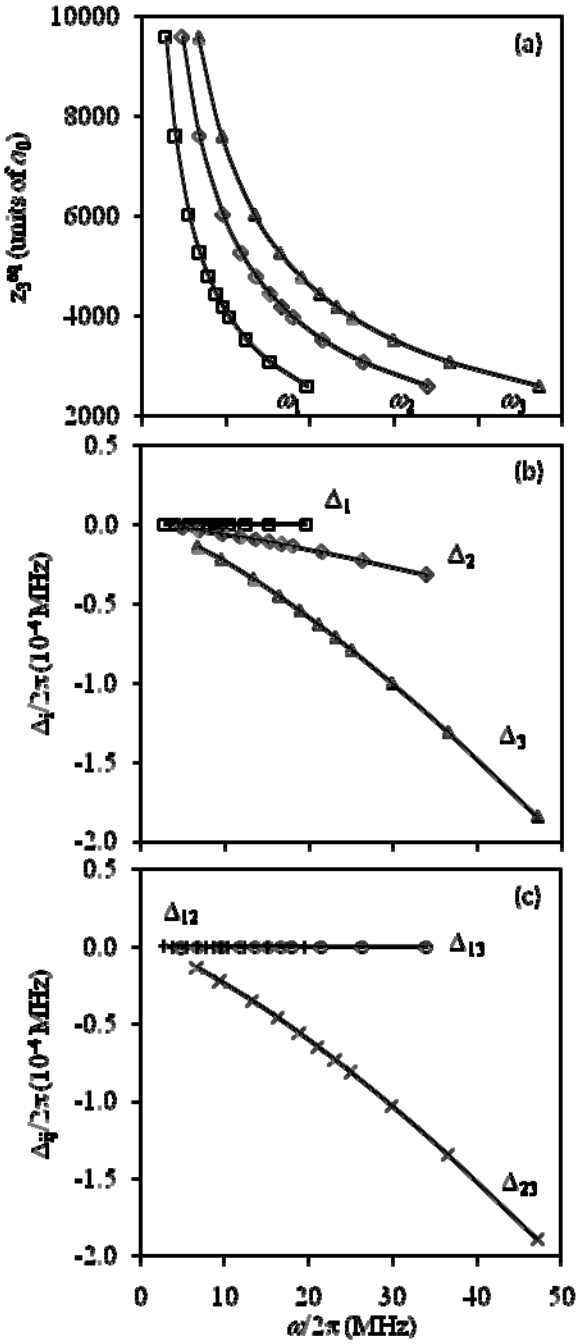

Fig. 7: Relations between the equilibrium distances, normal mode frequencies and vibrational anharmonicities for three ions in the harmonic potential trap.

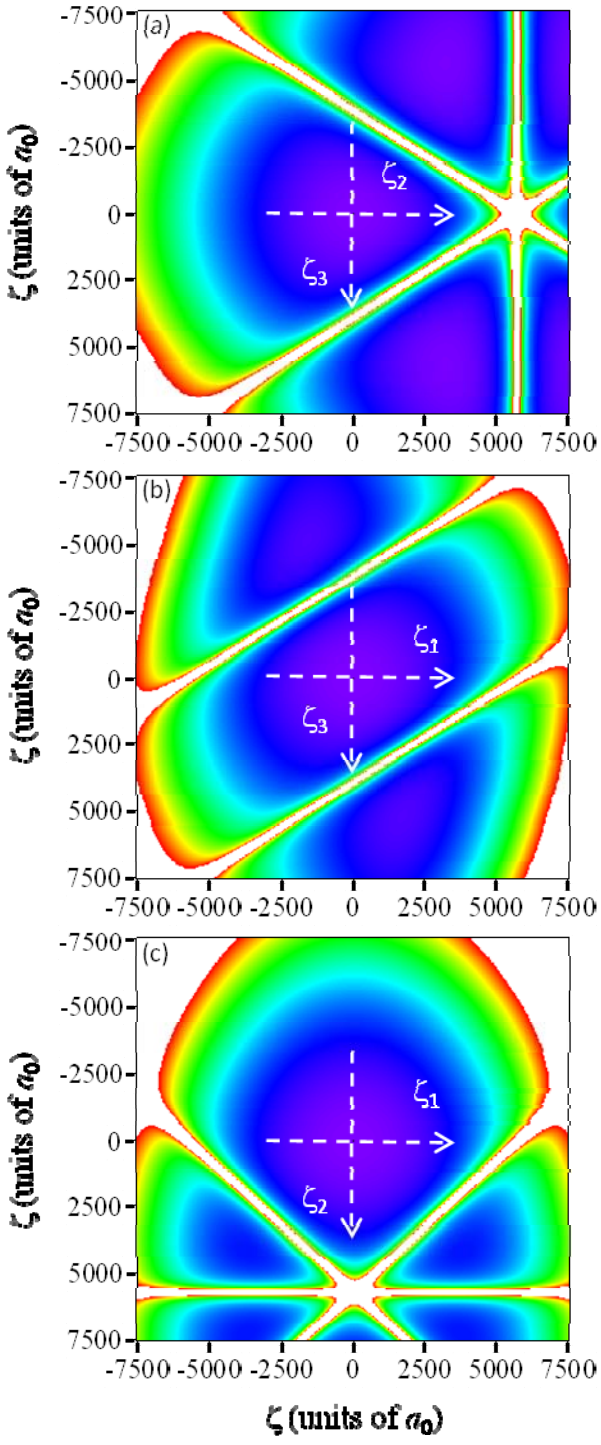

Fig. 8: Potential energy surface of three ions in the strongly anharmonic potential trap using the normal mode coordinates. Three slices through the 3D-surface are shown: *a*) perpendicular to ζ_1 through $\zeta_1 = 0$, *b*) perpendicular to ζ_2 through $\zeta_2 = 0$ and *c*) perpendicular to ζ_3 through $\zeta_3 = 0$.

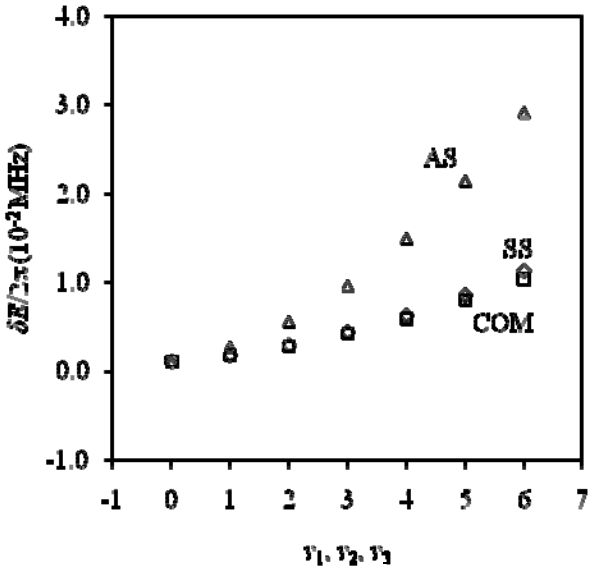

Fig. 9: Effect of anharmonicity on three modes of the vibrational spectrum of three ions in a strongly anharmonic ($\sim z^4$) potential trap -- the center-of-mass motion (COM) mode, the symmetric stretching (SS) mode and the asymmetric stretching (AS) mode.

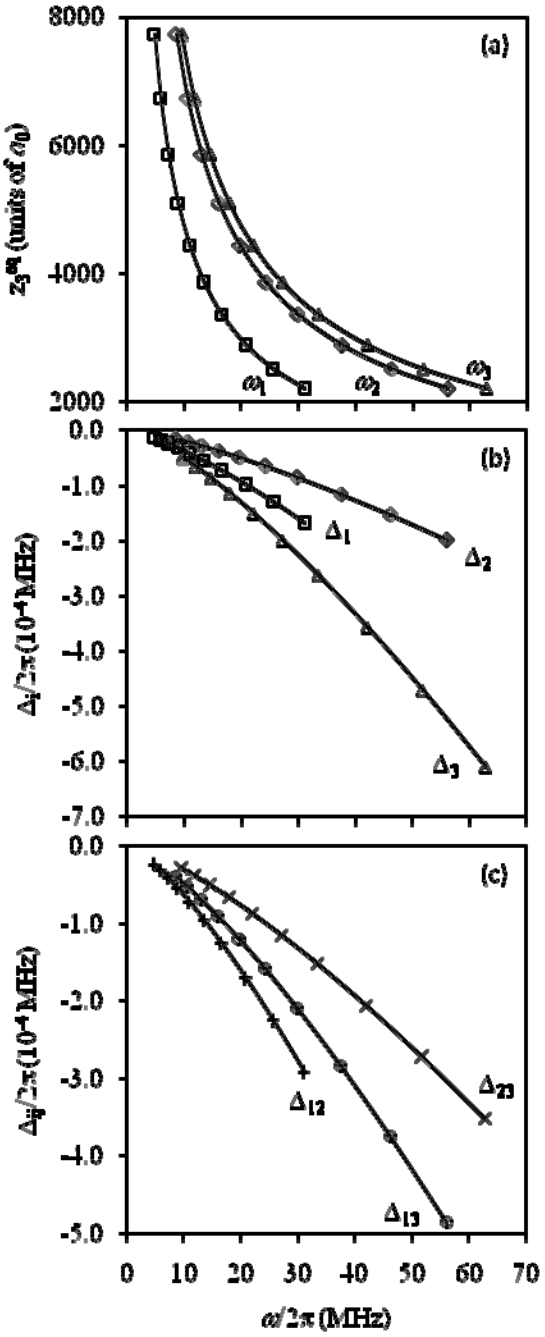

Fig. 10: Relations between the equilibrium distances, normal mode frequencies and vibrational anharmonicities for three ions in the strongly anharmonic potential trap.

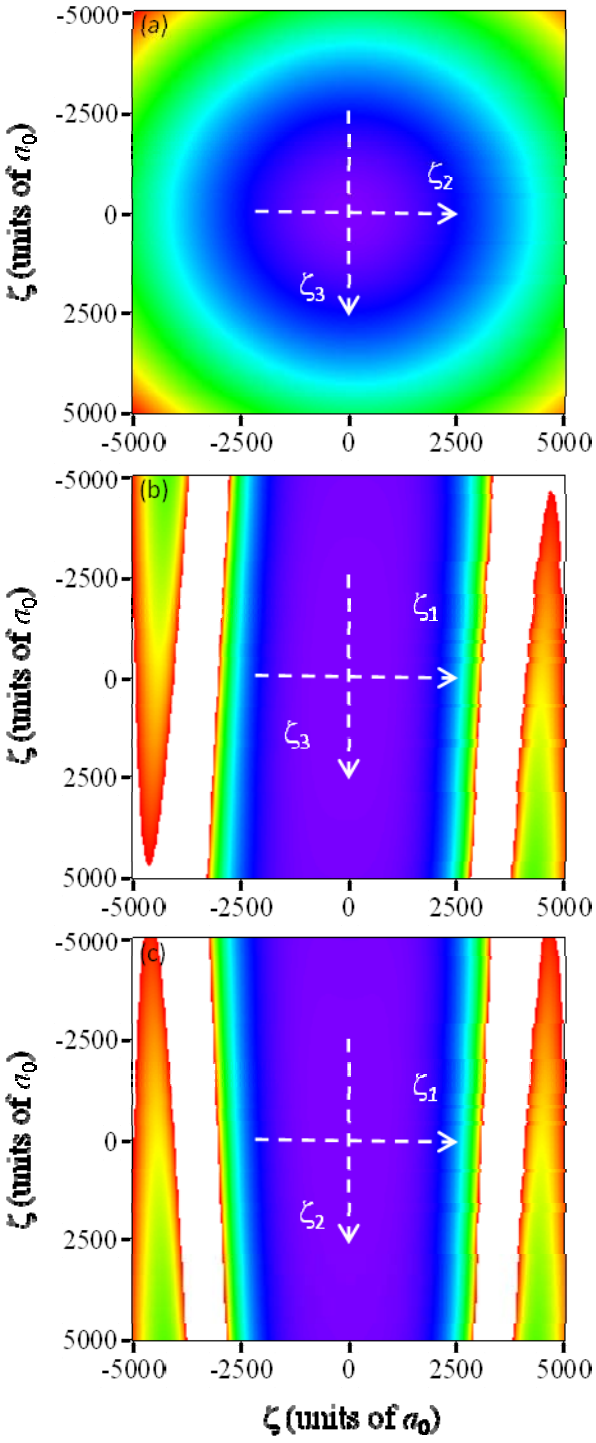

Fig. 11: Potential energy surface of three ions in the inverted combined potential trap using the normal mode coordinates. Three slices through the 3D-surface are shown: *a*) perpendicular to ζ_1 through $\zeta_1 = 0$, *b*) perpendicular to ζ_2 through $\zeta_2 = 0$ and *c*) perpendicular to ζ_3 through $\zeta_3 = 0$.

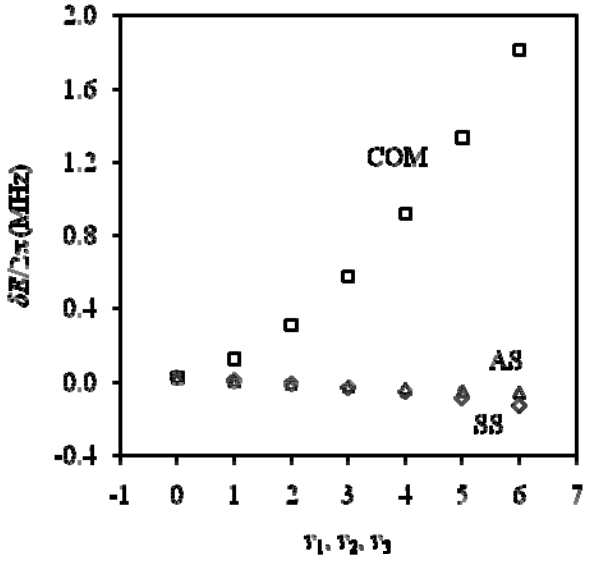

Fig. 12: Effect of anharmonicity on three modes of the vibrational spectrum of three ions in an inverted combined potential trap (with $\alpha = -100$ and $\beta = 1$) -- the center-of-mass motion (COM) mode, the symmetric stretching (SS) mode and the asymmetric stretching (AS) mode.

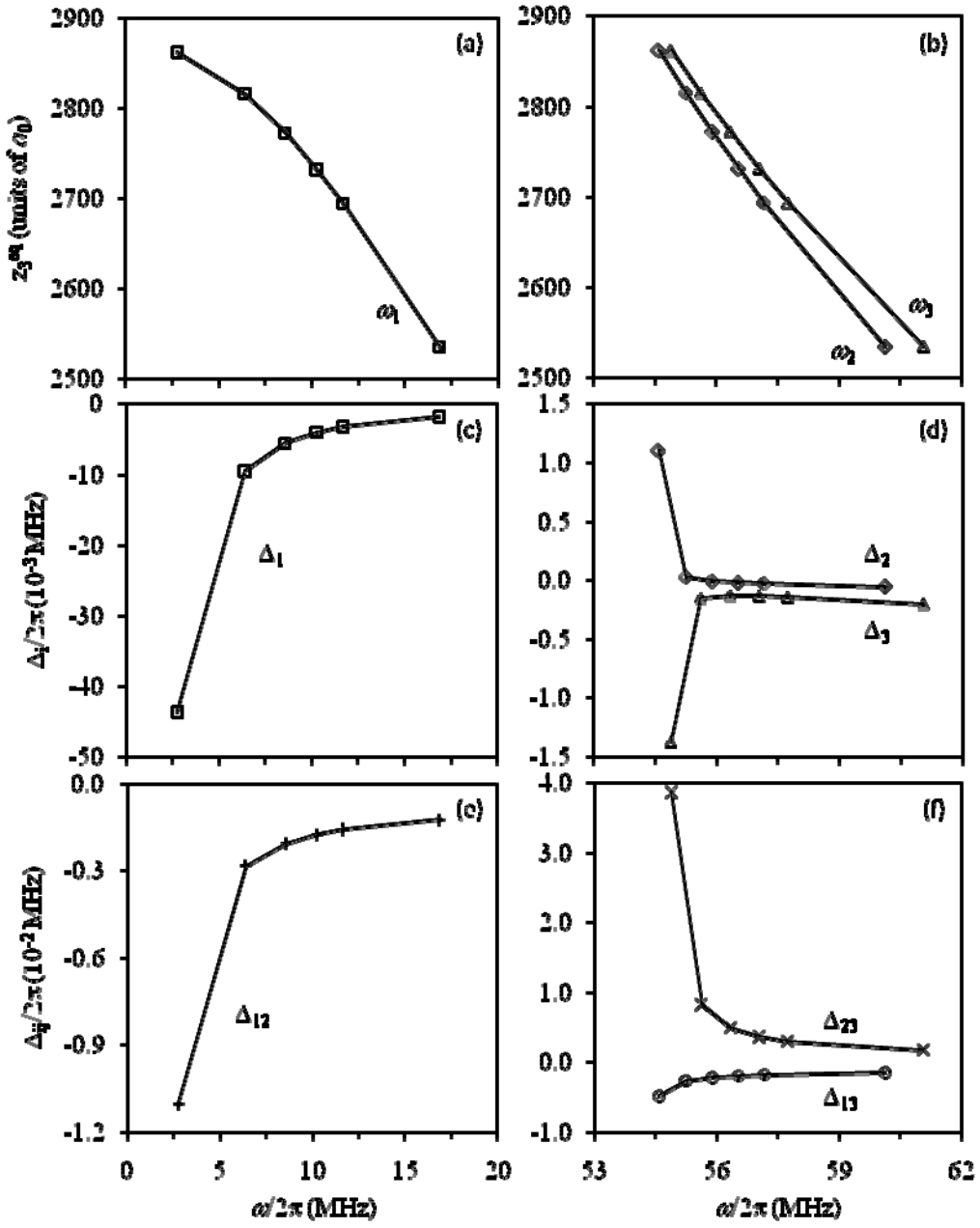

Fig. 13: Relations between the equilibrium distances, normal mode frequencies and vibrational anharmonicities for three ions in the inverted combined potential trap.

(Fig. 13: 1.5 columns)